Scalar meson contributions to a μ from hadronic light-by-light scattering

M. Knecht, S. Narison, A. Rabemananjara, D. Rabetiarivony

Physics Letters B 787 (2018) 111–123

Contents lists available at ScienceDirect

Physics Letters B

www.elsevier.com/locate/physletb

Scalar meson contributions to a_μ from hadronic light-by-light scattering

M. Knecht [a], S. Narison [b,*,1], A. Rabemananjara [c], D. Rabetiarivony [c,2]

[a] Centre de Physique Théorique UMR 7332, CNRS/Aix-Marseille Univ./Univ. du Sud Toulon-Var, CNRS Luminy Case 907, 13288 Marseille Cedex 9, France
[b] Laboratoire Particules et Univers de Montpellier, CNRS-IN2P3, Case 070, Place Eugène Bataillon, 34095 Montpellier, France
[c] Institute of High-Energy Physics (iHEPMAD), University of Antananarivo, Madagascar

ARTICLE INFO

Article history:
Received 14 August 2018
Received in revised form 11 October 2018
Accepted 23 October 2018
Available online 26 October 2018
Editor: A. Ringwald

Keywords:
Anomalous magnetic moment
Muon
Scalar mesons
Radiative width
Non perturbative effects

ABSTRACT

Using an effective $\sigma/f_0(500)$ resonance, which describes the $\pi\pi \to \pi\pi$ and $\gamma\gamma \to \pi\pi$ scattering data, we evaluate its contribution and the ones of the other scalar mesons to the hadronic light-by-light (HLbL) scattering component of the anomalous magnetic moment a_μ of the muon. We obtain the conservative range of values: $\sum_S a_\mu^{lbl}|_S \simeq -(4.51 \pm 4.12) \times 10^{-11}$, which is dominated by the $\sigma/f_0(500)$ contribution (50% ∼ 98%), and where the large error is due to the uncertainties on the parametrisation of the form factors. Considering our new result, we update the sum of the different theoretical contributions to a_μ within the standard model, which we then compare to experiment. This comparison gives $(a_\mu^{\rm exp} - a_\mu^{\rm SM}) = +(312.1 \pm 64.6) \times 10^{-11}$, where the theoretical errors from HLbL are dominated by the scalar meson contributions.

1. Introduction

The anomalous magnetic moments a_ℓ $(\ell \equiv e, \mu)$ of the light charged leptons, electron and muon, are among the most accurately measured observables in particle physics. The relative precision achieved by the latest experiments to date is of 0.28 ppb in the case of the electron [1,2], and 0.54 ppm in the case of the muon [3]. An ongoing experiment at Fermilab [4–6], and a planned experiment at J-PARC [7], aim at reducing the experimental uncertainty on a_μ to the level of 0.14 ppm, and there is also room for future improvements on the precision of a_e. The confrontation of these very accurate measurements with equally precise predictions from the standard model then provides a stringent test of the latter, and, as the experimental precision is further increasing, opens up the possibility of indirectly revealing physics degrees of freedom that even go beyond it.

From this last point of view, the present situation remains unconclusive in the case of the muon (in the case of the electron, the measured value of a_e agreed with the predicted value obtained from the measurement of the fine-structure constant of Ref. [8]; however, the more recent determination of α [9] now results in a tension at the level of 2.5 standard deviations between theory and experiment). Indeed, the latest standard model evaluations of a_μ (Ref. [10] provides a recent overview, as well as references to the literature; see also Section 10 at the end of this article) reveal a discrepancy between theory and experiment, which however is at the level of ∼ 3.5 standard deviations only. It is therefores mandatory, as the experimental precision increases, to also reduce the theoretical uncertainties in the evaluation of a_μ.

Presently, the limitation in the theoretical precision of a_μ is due to the contributions from the strong interactions, which are dominated by the low-energy, non perturbative, regime of quantum chromodynamics (QCD). The present work is devoted to a hadronic contribution arising at order $\mathcal{O}(\alpha^3)$, and currently refered to as hadronic light-by-light (HLbL), see Fig. 1. More precisely, we will be concerned with a particular contribution to HLbL, due to the exchange of the 0^{++} scalar states $\sigma/f_0(500)$, $a_0(980)$, $f_0(980)$, $f_0(1370)$, and $f_0(1500)$. In earlier evaluations of the HLbL part of a_μ, some of these states were either treated in the framework of the extended Nambu–Jona-Lasinio model [11,12], or they were simply omitted altogether [13,14]. More recently, in Ref. [15] the contributions from the $\sigma/f_0(500)$ and $a_0(980)$ scalars have been reconsidered in the framework of the linearized Nambu–Jona-Lasinio model. In Ref. [16], the contribution from the $a_0(980)$,

* Corresponding author.
E-mail addresses: marc.knecht@cpt.univ-mrs.fr (M. Knecht), snarison@yahoo.fr (S. Narison), achrisrab@gmail.com (A. Rabemananjara), rd.bidds@gmail.com (D. Rabetiarivony).

[1] Madagascar consultant of the Abdus Salam International Centre for Theoretical Physics (ICTP), via Beirut 6,34014 Trieste, Italy.

[2] PhD student.

https://doi.org/10.1016/j.physletb.2018.10.048

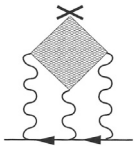

Fig. 1. Light-by-light Hadron scattering contribution to a_l. The wavy lines represent photon. The cross corresponds to the insertion of the electromagnetic current. The shaded box represents hadrons subgraphs.

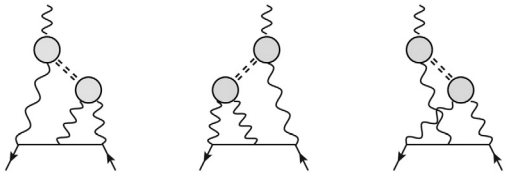

Fig. 2. Scalar meson exchange (dotted lines) to Light-by-light scattering contribution to a_μ. The wavy lines represent photon. The shaded blob represents form factors. The first and second diagrams contribute to the function T_1, and the third to the function T_2 defined in Eq. (3.11).

$f_0(980)$, $f_0(1370)$ states were evaluated as single-meson exchange terms with phenomenological form factors, see Fig. 2. Finally, the contribution from the lightest scalar, the $\sigma/f_0(500)$ is contained in the dispersive evaluation of the contribution to HLbL from two-pion intermediate states with $\pi\pi$ rescattering of Refs. [17,18].

The approach considered here for the treatment of the contribution from scalar states to HLbL has, to some extent, overlaps with both of the last two of these more recent approaches. It rests on a set of coupled-channel dispersion relations for the processes $\gamma\gamma \to \pi\pi, K\bar{K}$, where the strong S-matrix amplitudes for $\pi\pi \to \pi\pi, K\bar{K}$ are represented by an analytic K-matrix model, first introduced in Ref. [19], and gradually improved over time in Refs. [20–22], as more precise data on $\pi\pi$ scattering and on the reactions $\pi\pi \to \gamma\gamma$ became available. The details of the model will not be discussed here, as they are amply documented in the quoted references. The interest for our present purposes of the analysis of the data within this K-matrix framework is twofold. First, it contributes to our knowledge of the two-photon widths of some of the scalar states, which we will need as input. Second, through the fit to data of the K-matrix description of $\pi\pi$ scattering, it provides information on the mass and the total hadronic width of the $\sigma/f_0(500)$ resonance, which will also be needed.

The rest of this article is organized as follows. Section 2 briefly recalls the basic formalism describing the hadronic light-by-light contribution to the anomalous magnetic moment of a charged lepton. This is then specialized to the contribution due to the exchange of a narrow-width scalar state (Section 3). Some relevant properties of the vertex function involved are discussed in Section 4, where a vector-meson-dominance (VMD) representation satisfying its leading short-distance behaviour is also given. Three sections are devoted to a review of the properties (mass and width) of the f_0/σ scalar, coming either from sum rules (Section 6) or from phenomenology (Section 7). In Section 7 we furthermore describe how our formalism also allows to handle broad resonances like $\sigma/f_0(500)$ or $f_0(1370)$. The values of the mass and of the width of the $\sigma/f_0(500)$ retained for the present study are given in the last of these three sections (Section 8). The two-photon widths of the remaining scalar mesons are discussed in Section 9. Our results concerning the contributions of the scalars to HLbL are presented and discussed in Section 10. Finally, we summarize the present experimental and theoretical situation concerning the standard-model evaluation of the anomalous magnetic moment of the muon (Section 11) and end this article by giving our conclusions (Section 12).

2. Hadronic light-by-light contribution to a_l

The hadronic light-by-light contribution to the muon anomalous magnetic moment, illustrated in Fig. 1, is equal to [24]:

$$\begin{aligned} a_\mu^{lbl} &\equiv F_2(k=0) \\ &= \frac{1}{48m}\mathrm{tr}\left\{(\not{p}+m)[\gamma^\rho,\gamma^\sigma](\not{p}+m)\Gamma_{\rho\sigma}(p,p)\right\} \end{aligned} \tag{2.1}$$

where k is the momentum of the external photon, while m and p denote the muon mass and momentum. Furthermore $[p' = p + k]$

$$\begin{aligned} \Gamma_{\rho\sigma}(p',p) \equiv -ie^6 \int \frac{d^4q_1}{(2\pi)^4}\int \frac{d^4q_2}{(2\pi)^4}\frac{1}{q_1^2 q_2^2 (q_1+q_2-k)^2} \\ \times \frac{1}{(p'-q_1)^2-m^2}\,\frac{1}{(p'-q_1-q_2)^2-m^2} \\ \times \gamma^\mu(\not{p}'-\not{q}_1+m)\gamma^\nu(\not{p}'-\not{q}_1-\not{q}_2+m)\gamma^\lambda \\ \times \frac{\partial}{\partial k^\rho}\,\Pi_{\mu\nu\lambda\sigma}(q_1,q_2,k-q_1-q_2)\,, \end{aligned} \tag{2.2}$$

with q_1, q_2, q_3 the momenta or the virtual photons and

$$\begin{aligned} \Pi_{\mu\nu\lambda\rho}(q_1,q_2,q_3) = \int d^4x_1 \int d^4x_2 \int d^4x_3\, e^{i(q_1\cdot x_1+q_2\cdot x_2+q_3\cdot x_3)} \\ \times \langle 0|\mathrm{T}\{j_\mu(x_1)j_\nu(x_2)j_\lambda(x_3)j_\rho(0)\}|0\rangle \end{aligned} \tag{2.3}$$

the fourth-rank light quark vacuum polarization tensor, j_μ the electromagnetic current and $|0\rangle$ the QCD vacuum.

In practice, the computation of a_μ^{lbl} involves the limit $k \equiv p' - p \to 0$ of an expression of the type:

$$\begin{aligned} \mathcal{F}(p',p) = -ie^6 \int \frac{d^4q_1}{(2\pi)^4}\int \frac{d^4q_2}{(2\pi)^4}\,\mathcal{J}^{\mu\nu\rho\sigma\tau}(p',p;q_1,q_2) \\ \times \mathcal{F}_{\mu\nu\rho\sigma\tau}(-q_1,q_2+q_1+k,-q_2,-k), \end{aligned} \tag{2.4}$$

where

$$\begin{aligned} &\mathcal{J}^{\mu\nu\rho\sigma\tau}(p',p;q_1,q_2) \\ &= \frac{1}{(p'+q_1)^2-m^2}\,\frac{1}{(p-q_2)^2-m^2}\,\frac{1}{q_1^2 q_2^2 (q_1+q_2+k)^2} \\ &\quad\times \frac{1}{48m}\,\mathrm{tr}[(\not{p}+m)[\gamma^\sigma,\gamma^\tau](\not{p}'+m)\gamma^\mu(\not{p}'+\not{q}_1+m) \\ &\quad\times \gamma^\nu(\not{p}-\not{q}_2+m)\gamma^\rho]. \end{aligned} \tag{2.5}$$

This tensor has the symmetry property $\mathcal{J}^{\mu\nu\rho\sigma\tau}(p',p;q_1,q_2) = \mathcal{J}^{\rho\nu\mu\tau\sigma}(p,p';-q_2,-q_1)$, while, due to Lorentz invariance, $\mathcal{F}(p',p)$ depends on the momenta p and p' through their invariants only. For on-shell leptons, $p^2 = p'^2 = m^2$, this amounts to $\mathcal{F}(p',p) \equiv \mathcal{F}(k^2) = \mathcal{F}(p,p')$.

3. Scalar meson contributions to a_μ^{lbl}

Let us focus on the contribution to a_ℓ^{lbl} due to the exchange of a 0^{++} scalar meson S. We first discuss the situation where the width of this scalar meson is small enough so that its effects can be neglected. As a look to Table 1 shows, this will be the case for $S = a_0(980)$, $f_0(980)$, $f_0(1500)$. The circumstances under which the quite broad $\sigma/f_0(500)$ resonance, and possibly also the $f_0(1370)$ state, can be treated in a similar manner will be addressed in due course.

Table 1
The scalar states we consider together with the estimates or averages for the mass and width, as given by the 2018 Edition of the Review of Particle Physics [25]. In the cases of the $\sigma/f_0(500)$ and $f_0(1370)$ states, the ranges represent the estimates of the Breit–Wigner masses and widths.

Scalar	Mass [MeV]	Width [MeV]
$\sigma/f_0(500)$	400–550	400–700
$a_0(980)$	980(20)	50–100
$f_0(990)$	990(20)	10–100
$f_0(1370)$	1200–1500	200–500
$a_0(1450)$	1474(19)	265(13)
$f_0(1500)$	1504(6)	109(7)

The contribution $\Pi^{(S)}_{\mu\nu\rho\sigma}(q_1,q_2,q_3)$ due to the exchange of a scalar one-particle state $|S(p_S)\rangle$ to the fourth-order vacuum-polarization tensor $\Pi_{\mu\nu\rho\sigma}(q_1,q_2,q_3)$ (see Fig. 1) is described by the Feynman diagrams shown in Fig. 2. It involves the form factors describing the photon–photon-scalar vertex function

$$\begin{aligned}\Gamma^S_{\mu\nu}(q_1;q_2) &\equiv i\int d^4x e^{-iq_1\cdot x}\langle 0|T\{j_\mu(x)j_\nu(0)\}|S(p_S)\rangle \\ &= \mathcal{P}(q_1^2,q_2^2)P_{\mu\nu}(q_1,q_2)+\mathcal{Q}(q_1^2,q_2^2)Q_{\mu\nu}(q_1,q_2),\end{aligned} \tag{3.1}$$

where $q_2\equiv p_S-q_1$. This decomposition of $\Gamma^S_{\mu\nu}(q_1;q_2)$ follows from Lorentz invariance, invariance under parity, and the conservation of the current $j_\mu(x)$. The tensors

$$\begin{aligned}P_{\mu\nu}(q_1,q_2) &= q_{1,\nu}q_{2,\mu}-\eta_{\mu\nu}(q_1\cdot q_2),\\ Q_{\mu\nu}(q_1,q_2) &= q_2^2 q_{1,\mu}q_{1,\nu}+q_1^2q_{2,\mu}q_{2,\nu}\\ &\quad -(q_1\cdot q_2)q_{1,\mu}q_{2,\nu}-q_1^2q_2^2\eta_{\mu\nu},\end{aligned} \tag{3.2}$$

are transverse,

$$q^{\mu,\nu}_{1,2}P_{\mu\nu}(q_1,q_2)=0,\quad q^{\mu,\nu}_{1,2}Q_{\mu\nu}(q_1,q_2)=0, \tag{3.3}$$

and symmetric under the simultaneous exchanges of the momenta q_1 and q_2 and of the Lorentz indices μ and ν. The two off-shell scalar-photon–photon transition form factors $\mathcal{P}(q_1,q_2)$ and $\mathcal{Q}(q_1,q_2)$ depend only on the two independent invariants q_1^2 and q_2^2, and, are symmetric under permutation of the momenta q_1 and q_2. It is important to point out that the amplitude for the decay $S\to\gamma\gamma$, which is proportional to $\mathcal{P}(0,0)M_S^2(\epsilon_1\cdot\epsilon_2)$ [ϵ_i denote the respective photon polarization vectors, which are transverse, $q_i\cdot\epsilon_j=0$], provides information on $\mathcal{P}(0,0)$ only.

In order to simplify subsequent formulas, we will use the following short-hand notation:

$$P_{\mu\nu}(q_i,q_j)\equiv P^{(i,j)}_{\mu\nu},\quad Q_{\mu\nu}(q_i,q_j)\equiv Q^{(i,j)}_{\mu\nu}, \tag{3.4}$$

and

$$\begin{aligned}&\mathcal{P}(q_i^2,q_j^2)\equiv\mathcal{P}_{(i,j)}\quad;\quad \mathcal{P}[q_i^2,(q_j+q_k)^2]\equiv\mathcal{P}_{(i,jk)}\,,\\ &\mathcal{Q}(q_i^2,q_j^2)\equiv\mathcal{Q}_{(i,j)}\quad;\quad \mathcal{Q}[q_i^2,(q_j+q_k)^2]\equiv\mathcal{Q}_{(i,jk)}\,,\\ &\mathcal{P}(q_i^2,0)\equiv\mathcal{P}_{(i,0)}\quad;\quad \mathcal{Q}(q_i^2,0)\equiv\mathcal{Q}_{(i,0)}\,.\end{aligned} \tag{3.5}$$

The contribution $a_\mu^{lbl}|_S$ to a_μ^{lbl} from the exchange of the scalar S is then obtained upon replacing, in the general formula (2.3), the tensor $\Pi_{\mu\nu\rho\sigma}(q_1,q_2,q_3,q_4)$ by

$$\begin{aligned}&i\Pi^{(S)}_{\mu\nu\rho\sigma}(q_1,q_2,q_3,q_4)\\ &\quad=\mathcal{D}_S^{(1,2)}\left[\mathcal{P}_{(1,2)}P^{(1,2)}_{\mu\nu}+\mathcal{Q}_{(1,2)}Q^{(1,2)}_{\mu\nu}\right]\\ &\qquad\times\left[\mathcal{P}_{(3,4)}P^{(3,4)}_{\rho\sigma}+\mathcal{Q}_{(3,4)}Q^{(3,4)}_{\rho\sigma}\right]\\ &\qquad+\mathcal{D}_S^{(1,3)}\left[\mathcal{P}_{(1,3)}P^{(1,3)}_{\mu\rho}+\mathcal{Q}_{(1,3)}Q^{(1,3)}_{\mu\rho}\right]\\ &\qquad\times\left[\mathcal{P}_{(2,4)}P^{(2,4)}_{\nu\sigma}+\mathcal{Q}_{(2,4)}Q^{(2,4)}_{\nu\sigma}\right]\\ &\qquad+\mathcal{D}_S^{(1,4)}\left[\mathcal{P}_{(1,4)}P^{(1,4)}_{\mu\sigma}+\mathcal{Q}_{(1,4)}Q^{(1,4)}_{\mu\sigma}\right]\\ &\qquad\times\left[\mathcal{P}_{(2,3)}P^{(2,3)}_{\nu\rho}+\mathcal{Q}_{(2,3)}Q^{(2,3)}_{\nu\rho}\right]\\ &\quad\equiv i\left\{\Pi^{(S;PP)}_{\mu\nu\rho\sigma}+\Pi^{(S;PQ)}_{\mu\nu\rho\sigma}+\Pi^{(S;QQ)}_{\mu\nu\rho\sigma}\right\},\end{aligned} \tag{3.6}$$

where $q_4^\mu\equiv-(q_1+q_2+q_3)^\mu$. The scalar-meson propagator in the Narrow Width Approximation (NWA) reads

$$\mathcal{D}_S^{(i)}\equiv\frac{1}{q_i^2-M_S^2}\,;\quad \mathcal{D}_S^{(i,j)}\equiv\frac{1}{(q_i+q_j)^2-M_S^2}\,, \tag{3.7}$$

with $i,j=1,..4$. In the last line, the first (third) term collects all the contributions quadratic in the form factor $\mathcal{P}$ ($\mathcal{Q}$), while the second term collects all the contributions involving the products $\mathcal{P}\mathcal{Q}$ of the two kinds of form factors. Correspondingly, we perform the decomposition $a_\mu^{lbl}|_S=a_\mu^{lbl}|_S^{PP}+a_\mu^{lbl}|_S^{PQ}+a_\mu^{lbl}|_S^{QQ}$.

Starting from the representation (3.6), it is a straightforward exercise to insert it into the general expression in Eq. (2.3), and then to compute the projection on the Pauli form factor as defined in Eq. (2.1). For further use, we introduce the tensor $\mathcal{F}_{\mu\alpha\beta}(q)=\eta_{\mu\beta}q_\alpha-\eta_{\mu\alpha}q_\beta$, and the amplitude

$$A_S^{PP}(q_1,q_2,q_3,q_4)\equiv\mathcal{D}_S^{(1,2)}\mathcal{P}_{(1,2)}\mathcal{P}_{(3,4)}, \tag{3.8}$$

and similarly for other products of form factors PQ, QQ.

The part of the scalar-exchange term that involves the form factor $\mathcal{P}$ alone then reads

$$\begin{aligned}a_\mu^{lbl}|_S^{PP}=-e^6\int\frac{d^4q_1}{(2\pi)^4}\int\frac{d^4q_2}{(2\pi)^4}\mathcal{J}^{\mu\nu\rho\sigma\tau}(p,p;q_1,q_2)\\ \times\Big\{2A_S^{PP}(-q_1,q_1+q_2,-q_2,0)\mathcal{F}_{\mu\nu\alpha}(q_1)(q_1+q_2)^\alpha\\ \times\mathcal{F}_{\rho\sigma\tau}(q_2)+A_S^{PP}(-q_1,-q_2,q_1+q_2,0)\\ \times\mathcal{F}_{\mu\rho\alpha}(q_1)q_2^\alpha\mathcal{F}_{\nu\sigma\tau}(q_1+q_2)\Big\},\end{aligned} \tag{3.9}$$

where the symmetry properties of the integrand, and of the amplitude $A_S(q_1,q_2,q_3,q_4)$, as well as $\mathcal{F}_{\rho\sigma\tau}(q)=-\mathcal{F}_{\rho\tau\sigma}(q)$ have been used. Noticing that $Q_{\mu\nu}(q,k)$ is quadratic in the components of the momentum k^μ, one sees that all of $\Pi^{(S;QQ)}_{\mu\nu\rho\sigma}(q_1,q_2,q_3)$ and half of the terms in $\Pi^{(S;PQ)}_{\mu\nu\rho\sigma}(q_1,q_2,q_3)$ will not contribute to the Pauli form factor at vanishing momentum transfer. The part of the scalar-exchange term that involves both form factors $\mathcal{P}$ and $\mathcal{Q}$ thus reduces to

$$\begin{aligned}a_\mu^{lbl}|_S^{PQ}=-e^6\int\frac{d^4q_1}{(2\pi)^4}\int\frac{d^4q_2}{(2\pi)^4}\mathcal{J}^{\mu\nu\rho\sigma\tau}(p,p;q_1,q_2)\\ \times\Big\{2A_S^{PQ}(-q_2,0,-q_1,q_1+q_2)\mathcal{F}_{\rho\sigma\tau}(-q_2)\\ \times Q_{\mu\nu}(q_1,q_1+q_2)+A_S^{PQ}(q_1+q_2,0,q_1,q_2)\\ \times\mathcal{F}_{\nu\sigma\tau}(q_1+q_2)Q_{\mu\rho}(q_1,q_2)\Big\},\end{aligned} \tag{3.10}$$

whereas $a_\mu^{lbl}|_S^{QQ}=0$. The trace calculation[3] leads to the final expression

[3] The corresponding Dirac traces have been computed using the FeynCalc package [26,27].

$$a_\mu^{lbl}|_S = -e^6 \int \frac{d^4q_1}{(2\pi)^4} \int \frac{d^4q_2}{(2\pi)^4} \times \frac{1}{q_1^2 q_2^2 (q_1+q_2)^2} \frac{1}{(p+q_1)^2 - m^2} \frac{1}{(p-q_2)^2 - m^2} \Big\{ \mathcal{D}_S^{(2)} \big[\mathcal{P}_{(1,12)} \mathcal{P}_{(2)}\, T_{1,S}^{PP} + \mathcal{P}_{(2)} \mathcal{Q}_{(1,12)}\, T_{1,S}^{PQ} \big] + \mathcal{D}_S^{(1,2)} \big[\mathcal{P}_{(1,2)} \mathcal{P}_{(12,0)}\, T_{2,S}^{PP} + \mathcal{P}_{(12,0)} \mathcal{Q}_{(12,0)}\, T_{2,S}^{PQ} \big] \Big\}, \tag{3.11}$$

where the amplitudes $T_{i,S}$ are given in Table 2 and the functions $\mathcal{P}_{(i,j)}$ and $\mathcal{Q}_{(i,j)}$ in Eq. (3.5). Let us simply note here that $T_1^{(PP)}(q_1,q_2)$ and $T_1^{(PQ)}(q_1,q_2)$ come from the sum of the two diagrams (*a*) and (*b*) of Fig. 2 (they give identical contributions), while $T_2^{(PP)}(q_1,q_2)$ and $T_2^{(PQ)}(q_1,q_2)$ represent the contributions from diagram (*c*). Apart from the presence of two form factors, the situation, at this level, is similar to the one encountered in the case of the exchange of a pseudoscalar meson, see for instance Ref. [28].

4. $\Gamma^S_{\mu\nu}$ at short distance and vector meson dominance

In order to proceed, some information about the vertex function $\Gamma^S_{\mu\nu}(q, p_S - q)$ is required. In particular, the question about the relative sizes of the contributions to $a_\mu^{lbl}|_S$ coming from the two form factors involved in the description of the matrix element (3.1) needs to be answered. In order to briefly address this issue, one first notices that at short distances the vertex function $\Gamma^S_{\mu\nu}(q, p_S - q)$ has the following behaviour (in the present discussion q^μ is a spacelike momentum):

$$\lim_{\lambda\to\infty} \Gamma^S_{\mu\nu}(\lambda q, p_S - \lambda q) = \frac{1}{\lambda^2} \left(\frac{1}{q^2}\right)^2 \Gamma^{S;\infty}_{\mu\nu}(q, p_S) + \mathcal{O}\left(\frac{1}{\lambda^2}\right)^3, \tag{4.1}$$

with

$$\Gamma^{S;\infty}_{\mu\nu}(q, p_S) = (q_\mu q_\nu - q^2 \eta_{\mu\nu}) A + \big[(q\cdot p_S) q_\mu p_{S,\nu} - q^2 p_{S,\mu} p_{S,\nu} + (q\cdot p_S)(q_\nu p_{S,\mu} - q\cdot p_S \eta_{\mu\nu}) \big] B. \tag{4.2}$$

The structure of $\Gamma^{S;\infty}_{\mu\nu}(q, p_S)$ follows from the requirements $q^\mu \Gamma^{S;\infty}_{\mu\nu}(q, p_S) = 0$, $q^\nu \Gamma^{S;\infty}_{\mu\nu}(q, p_S) = 0$, and the coefficients A and B are combinations of the four independent "decay constants" which describe the matrix elements

$$\langle 0| : D_\rho \bar\psi Q^2 \gamma_\sigma \psi : (0) |S(p_S)\rangle,\ \langle 0| : \bar\psi Q^2 \mathcal{M} \psi : (0) |S(p_S)\rangle,$$
$$\langle 0| : G^a_{\mu\nu} G^a_{\rho\sigma} : (0) |S(p_S)\rangle, \tag{4.3}$$

of the three gauge invariant local operators of dimension four that can couple to the 0^{++} scalar states. Here $Q = \mathrm{diag}(2/3, -1/3, -1/3)$ denotes the charge matrix of the light quarks, whereas $\mathcal{M} = \mathrm{diag}(m_u, m_d, m_s)$ stands for their mass matrix. The third matrix element, involving the gluonic operator $: G^a_{\mu\nu} G^a_{\rho\sigma} :$, only occurs to the extent that the scalar state possesses a singlet component. For a pure octet state, and in the chiral limit, only one "decay constant", coming from the first operator, remains, and one has $A/B = -M_S^2/2$. The asymptotic behaviour in Eq. (4.2) leads to the suppression of $\mathcal{Q}(q_1,q_2)$ with respect to $\mathcal{P}(q_1,q_2)$ at high (spacelike) photon virtualities ($Q_i^2 = -q_i^2$):

$$\mathcal{Q}(q_1,q_2) \simeq -\frac{2\mathcal{P}(q_1,q_2)}{Q_1^2 + Q_2^2}. \tag{4.4}$$

This short-distance behaviour can be reproduced by a simple vector meson dominance (VMD)-type representation,

$$\mathcal{P}^{\mathrm{VMD}}(q_1,q_2) = -\frac{1}{2} \frac{B(q_1^2+q_2^2) + (2A + M_S^2 B)}{(q_1^2 - M_V^2)(q_2^2 - M_V^2)},$$
$$\mathcal{Q}^{\mathrm{VMD}}(q_1,q_2) = -\frac{B}{(q_1^2 - M_V^2)(q_2^2 - M_V^2)}, \tag{4.5}$$

which leads to:

$$\kappa_S \equiv -\frac{M_S^2 \mathcal{Q}^{\mathrm{VMD}}(0,0)}{\mathcal{P}^{\mathrm{VMD}}(0,0)} = -\frac{2BM_S^2}{BM_S^2 + 2A}. \tag{4.6}$$

Incidentally, similar statements can also be inferred from Ref. [29], where the octet vector–vector-scalar three-point function $\langle VVS\rangle$ was studied in the chiral limit. From the expressions given there, one obtains

$$\frac{M_S^2 \mathcal{Q}(q_1,q_2)}{\mathcal{P}(q_1,q_2)} = -\left[\frac{9}{5} \frac{M_V^4}{F_\pi^2 (M_K^2 - M_\pi^2)} \tilde c - \frac{1}{2} + \frac{Q_1^2 + Q_2^2}{2M_S^2} \right]^{-1} \simeq -\frac{2M_S^2}{2M_S^2 + Q_1^2 + Q_2^2}, \tag{4.7}$$

with [30]

$$\tilde c = \frac{5}{16\pi\alpha^2} \left[\frac{\Gamma_{\rho\to e^+e^-}}{M_\rho} - 3\frac{\Gamma_{\omega\to e^+e^-}}{M_\omega} - 3\frac{\Gamma_{\phi\to e^+e^-}}{M_\phi} \right] \simeq (4.6 \pm 0.8)\cdot 10^{-3}. \tag{4.8}$$

Numerically, this would correspond to $A/B = -2M_S^2$ ($\kappa_S = 1$), rather than to $A/B = -M_S^2/2$, which, as mentioned above, should hold precisely for the conditions under which the analysis carried out in Ref. [29] is valid. This discrepancy illustrates the well-known [31,32] limitation of the simple saturation by a single resonance in each channel, which in general cannot simultaneously accommodate the correct short-distance behaviour of a given correlator and of the various related vertex functions. Let us also point out that $A/B = -M_S^2/2$ corresponds to $\mathcal{P}(0,0) = 0$, i.e. to a vanishing two-photon width. This either means that scalars without a singlet component decay into two photons through quark-mass and/or through isospin-violating effects, or, more likely, shows the limitation of the VMD picture, which provides, in this case, a too simplistic description of a more involved situation. The second alternative would then require to go beyond a single-resonance description, as described, for instance, in Ref. [32] for the photon-transition form factor of the pseudoscalar mesons. Following this path would, however, lead us too far astray, and in the present study we will keep the discussion within the framework set by the VMD description of the two form factors $\mathcal{P}(q_1,q_2)$ and $\mathcal{Q}(q_1,q_2)$. For later use, like for instance the derivation of Eq. (5.4) below, it is also of interest to parameterize the VMD form factors directly in terms of $\mathcal{P}(0,0)$, which gives the two-photon width, and the parameter κ_S as defined by the first equality in Eq. (4.6):

$$\mathcal{P}^{VMD}(q_1,q_2) = \mathcal{P}(0,0) \left[1 - \frac{\kappa_S}{2} \frac{q_1^2 + q_2^2}{M_S^2} \right] \times \frac{M_V^4}{(q_1^2 - M_V^2)(q_2^2 - M_V^2)},$$
$$\mathcal{Q}^{VMD}(q_1,q_2) = -\kappa_S \frac{\mathcal{P}(0,0)}{M_S^2} \frac{M_V^4}{(q_1^2 - M_V^2)(q_2^2 - M_V^2)}. \tag{4.9}$$

Table 2
Expressions, in Minkowski space, of the amplitudes defined in Eq. (3.11).

$$T^{PP}_{1,S}(q_1,q_2) = \frac{16}{3}\Big[q_2^2(p\cdot q_1)^2 + q_1^2(p\cdot q_2)^2 - (q_1\cdot q_2)(p\cdot q_1)(p\cdot q_2) + (p\cdot q_1)(p\cdot q_2)q_2^2 + (p\cdot q_1)(q_1\cdot q_2)q_2^2 - (p\cdot q_2)(q_1\cdot q_2)^2 - m_\ell^2 q_1^2 q_2^2 - m_\ell^2 (q_1\cdot q_2)q_2^2\Big]$$
$$+ 8(p\cdot q_1)q_1^2 q_2^2 - 8q_1^2(p\cdot q_2)(q_1\cdot q_2),$$
$$T^{PP}_{2,S}(q_1,q_2) = \frac{8}{3}\Big[q_2^2(p\cdot q_1)^2 + q_1^2(p\cdot q_2)^2 - 2(q_1+q_2)^2(p\cdot q_1)(p\cdot q_2) + (p\cdot q_1)(p\cdot q_2)q_1^2 + (p\cdot q_1)(p\cdot q_2)q_2^2 + m^2(q_1\cdot q_2)(q_1+q_2)^2\Big].$$
$$T^{PQ}_{1,S}(q_1,q_2) = \frac{16}{3}\Big[(q_1\cdot q_2)(p\cdot q_1)(p\cdot q_2)(q_1^2+q_2^2) + (p\cdot q_1)(p\cdot q_2)(q_1\cdot q_2)^2 + (p\cdot q_2)(q_1\cdot q_2)q_1^2 q_2^2 - q_1^2 q_2^2 (p\cdot q_1)^2 -$$
$$q_1^2 q_2^2 (p\cdot q_2)^2 - q_2^2(q_1\cdot q_2)(p\cdot q_1)^2 - q_1^2(q_1\cdot q_2)(p\cdot q_2)^2 - (p\cdot q_1)^2 q_2^4 - (p\cdot q_2)^2 q_1^4 - (p\cdot q_1)q_1^2 q_2^4 -$$
$$(p\cdot q_1)(p\cdot q_2)q_1^2 q_2^2 + m_\ell^2 q_1^2 q_2^2 (q_1+q_2)^2\Big] - \frac{40}{3}\Big[(p\cdot q_1)(q_1\cdot q_2)q_1^2 q_2^2 - (p\cdot q_2)(q_1\cdot q_2)^2 q_1^2\Big] + 8q_1^4\big[(p\cdot q_2)(q_1\cdot q_2) - q_2^2(p\cdot q_1)\big],$$
$$T^{PQ}_{2,S}(q_1,q_2) = \frac{4}{3}\Big[2(q_1\cdot q_2)(p\cdot q_1)(p\cdot q_2)(q_1^2+q_2^2) - q_2^2(q_1+q_2)^2(p\cdot q_1)^2 - q_1^2(q_1+q_2)^2(p\cdot q_2)^2 - q_2^2(q_1^2+q_2^2)(p\cdot q_1)^2 - q_1^2(q_1^2+q_2^2)(p\cdot q_2)^2 + 2m_\ell^2 q_1^2 q_2^2 (q_1+q_2)^2\Big].$$

We may draw two conclusions from the preceding analysis. First, that a sensible comparison to be made, for space-like photon virtualities, is thus not between $\mathcal{P}(q_1,q_2)$ and $\mathcal{Q}(q_1,q_2)$, but rather between $\mathcal{P}(q_1,q_2)$ and, say, $-(2M_S^2+Q_1^2+Q_2^2)\mathcal{Q}(q_1,q_2)/2$. At high photon virtualities, their ratio tends to unity. Second, that $|\mathcal{P}(0,0)|$ and $M_S^2|\mathcal{Q}(0,0)|$ may well be of comparable sizes. For instance, within VMD, we obtain

$$\mathcal{P}(0,0) = -M_S^2\mathcal{Q}(0,0) \tag{4.10}$$

from the analysis of Ref. [29].

5. Angular integrals

The next step consists in transforming the two-loop integral in Eq. (3.11) into an integration in Euclidian space through the replacement

$$\int d^4q_i \longrightarrow i(2\pi^2)\int_0^\infty dQ_i\, Q_i^3 \int \frac{d\Omega_{\hat{Q}_i}}{2\pi^2}, \tag{5.1}$$

with $Q_i^2 = -q_i^2$, $i=1,2$, and

$$d\Omega_{\hat{Q}_i} = d\phi_{\hat{Q}_i} d\theta_{1\hat{Q}_i} d\theta_{2\hat{Q}_i} \sin(\theta_{1\hat{Q}_i})\sin^2(\theta_{2\hat{Q}_i}),$$
$$\int d\Omega_{\hat{Q}_i} = 2\pi^2, \tag{5.2}$$

where the orientation of the four-vector Q_μ in four-dimensional Euclidian space is given by the azymuthal angle $\phi_{\hat{Q}}$ and the two polar angles $\theta_{1\hat{Q}}$ and $\theta_{2\hat{Q}}$. Since the anomalous magnetic moment is a Lorentz invariant, its value does not depend on the lepton's four-momentum p^μ beyond its mass-shell condition $p^2 = m^2$. One may thus average, in Euclidian space, over the directions of the four-vector P (the Euclidian counterpart of p, i.e. $P^2 = -m^2$)

$$a_\mu^{lbl}|_S = \frac{1}{2\pi^2}\int d\Omega_{\hat{P}}\, a_\mu^{lbl}|_S. \tag{5.3}$$

This allows to obtain a representation of $a_\mu^{lbl}|_S^{PP+PQ}$ as an integral over three variables, Q_1, Q_2, and the angle between the two Euclidian loop momenta [33]. Actually, in the VMD representation of Eq. (4.5), the form factors belong to the general class discussed in Ref. [28], for which one can actually perform the angular integrals directly, without having to average over the direction of the lepton four-momentum first. Within this VMD approximation of the form factors, the anomalous magnetic moment then reads

$$a_\mu^{lbl}|_S^{\rm VMD} = \left(\frac{\alpha}{\pi}\right)^3 [\mathcal{P}(0,0)]^2 \int_0^\infty dQ_1 \int_0^\infty dQ_2$$
$$\frac{M_V^4}{(Q_1^2+M_V^2)(Q_2^2+M_V^2)}$$
$$\Bigg\{\Big[\Delta w_1^{PP}(M_V) - \Delta w_2^{PP}(M_V)\Big]$$
$$+ \frac{\kappa_S}{2}\Bigg\{\frac{Q_1^2+Q_2^2}{M_S^2}\Big[\Delta w_1^{PP}(M_V) - \Delta w_2^{PP}(M_V)\Big]$$
$$- \frac{M_V^2}{M_S^2}\Big[w_{12}^{PP}(M_V) - 2\Delta w_1^{PQ}(M_V) - 2\Delta w_2^{PQ}(M_V)\Big]\Bigg\}$$
$$+ \frac{\kappa_S^2}{4}\Bigg[\frac{Q_1^2Q_2^2}{M_S^4}\Delta w_1^{PP}(M_V) - \tilde{w}_{12}^{PP}(M_V)$$
$$- 2\frac{Q_2^2}{M_S^2}\Delta w_1^{PQ}(M_V) - 2\frac{Q_1^2+Q_2^2}{M_S^2}\Delta w_2^{PQ}(M_V)\Bigg]\Bigg\}$$
$$\equiv \left(\frac{\alpha}{\pi}\right)^3 [\mathcal{P}(0,0)]^2\Big\{\mathcal{I}_p + \kappa_S\mathcal{I}_{pq} + \kappa_S^2\mathcal{I}_q\Big\}, \tag{5.4}$$

where κ_S was defined in Eq. 4.6, and with

$$\Delta w_{1,2}^{PP,PQ}(M) \equiv w_{1,2}^{PP,PQ}(M) - w_{1,2}^{PP,PQ}(0), \tag{5.5}$$
$$w_{12}^{PP}(M_V) = w_1^{PP}(M_V) - w_2^{PP}(M_V), \tag{5.6}$$
$$\tilde{w}_{12}^{PP}(M_V) = \frac{Q_2^2M_V^2}{M_S^4}w_1^{PP}(M_V) - \frac{Q_1^2+Q_2^2}{M_S^2}\frac{M_V^2}{M_S^2}w_2^{PP}(M_V).$$

The dimensionless densities (the overall sign has been chosen such that these densities are positive) occurring in these expressions can be found in Table 3. They are obtained upon using the angular integrals given in [28]. Some of their combinations are plotted in Figs. 3, 4, and 5. Generically, they are peaked in a region around $Q_1 \sim Q_2 \sim 500$ MeV, and are suppressed for smaller or larger values of the Euclidian loop momenta.

6. $I = 0$ scalar mesons from gluonium sum rules

The evaluation of $a_\mu^{lbl}|_S^{\rm VMD}$ as given in Eq. (5.4), requires as input values for the masses and the two-photon widths of the various scalar resonances we want to include. For the narrow states, this information can be gathered from the review [25] or from other sources, which will be described in Section 9. In this section, we review the information provided by various QCD spectral sum rules and some low-energy theorems on the mass, as well as on the hadronic and two-photon widths, of the lightest scalar meson $\sigma/f_0(500)$, the $f_0(1350)$ and $f_0(1504)$ interpreted as gluonia states.

- *$I = 0$ scalar mesons as gluonia candidates*

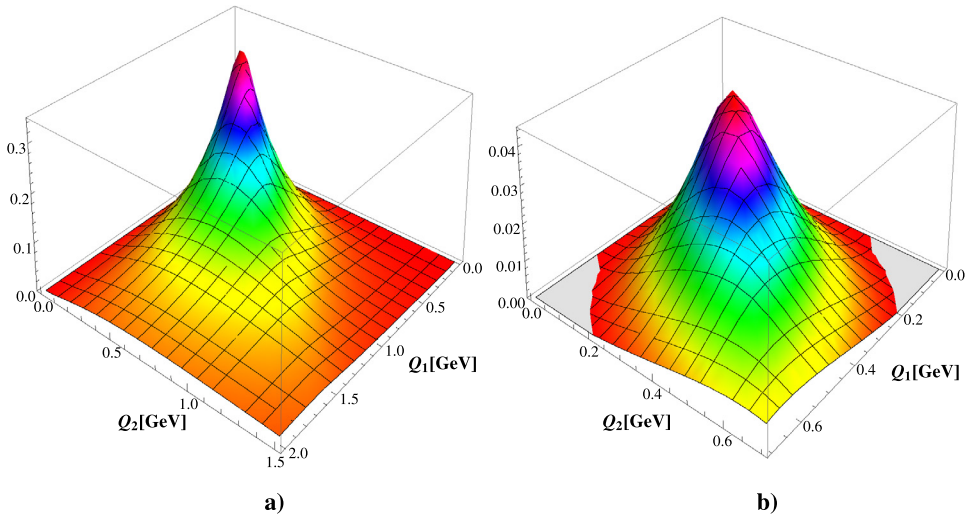

Fig. 3. The weight functions: **a)**: Δw_1^{PP} and **b)**: Δw_2^{PP} as function of Q_1 and Q_2. We have used $M_V = M_\rho = 775$ MeV and $M_S = 960$ MeV.

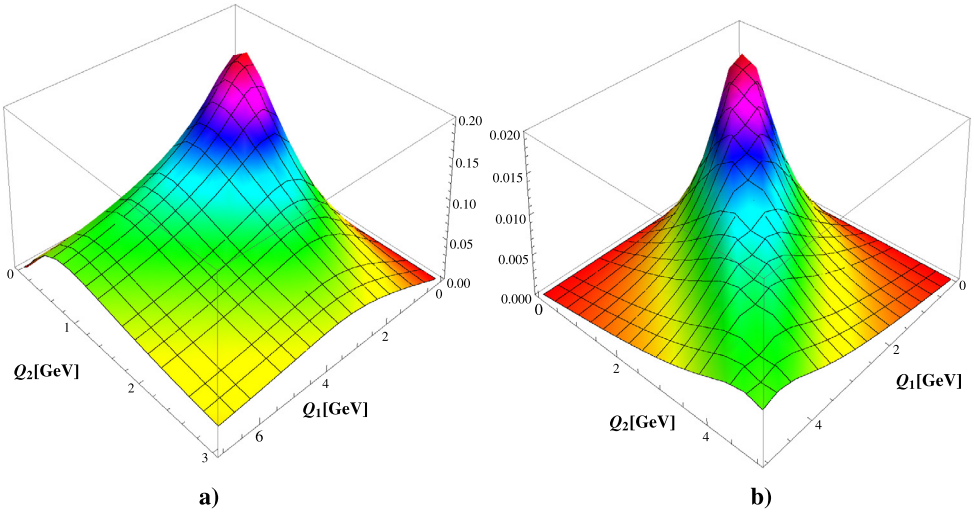

Fig. 4. The same as in Fig. 3 but for PQ.

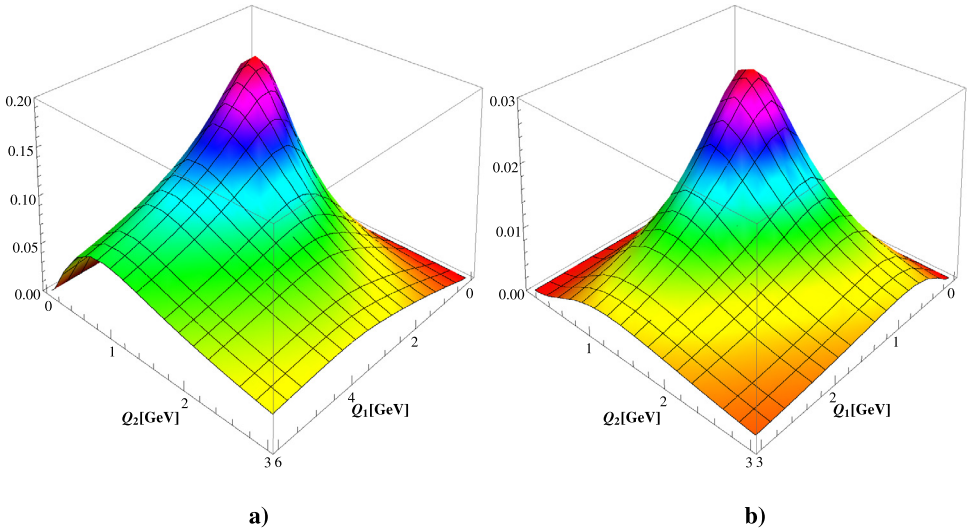

Fig. 5. The same as in Fig. 3 but for the combinations w_{12}^{PP} and $\tilde{w}_{12}^{PP}$ in Eq. (5.6).

The nature of the isoscalar $I = 0$ scalar states remains unclear as it goes beyond the usual octet quark model description due to their $U(1)$ component. A four-quark description of these states have been proposed within the bag model [34] and studied phenomenologically in e.g. Refs. [35,36]. However, its singlet nature has also motivated their interpretation as gluonia candidates as initiated in Ref. [37] and continued in Refs. [38–42].[4] Recent analysis of the $\pi\pi$ and $\gamma\gamma$ scattering data indicates an eventual large gluon component of the $\sigma/f_0(500)$ and $f_0(990)$ states [19–23] while recent data analysis from central productions [47] shows the gluonium nature of the $f_0(1350)$ decaying into $\pi^+\pi^-$ and into the specific $4\pi^0$ states via two virtual $\sigma/f_0(500)$ states as expected if it is a gluonium [40,41]. The $\sigma/f_0(500)$ are observed in the gluonia golden J/ψ and $\Upsilon \to \pi\pi\gamma$ radiative decays but often interpreted as S-wave backgrounds due to its large width (see e.g. BESIII [48] and BABAR [49]). The glueball nature of the $G(1.5-1.6)$ has been also found by GAMS few years ago [50] on its decay to $\eta'\eta$ and on the value of the branching ratio $\eta'\eta/\eta\eta$ expected for a high-mass gluonium [40,41].

- *The σ/f_0 mass from QCD spectral sum rules*

The singlet nature of the σ/f_0 has motivated to consider that it may contain a large gluon component [39–41], which may explain its large mass compared to the pion. This property is encoded in the trace of the QCD energy momentum tensor:

$$\theta^\mu_\mu = \frac{1}{4}\beta(\alpha_s) G^a_{\mu\nu} G^{\mu\nu}_a + \big[1+\gamma_m(\alpha_s)\big]\sum_{u,d,s} m_q \bar\psi_q \psi_q, \tag{6.1}$$

where $\beta(\alpha_s) \equiv \beta_1(\alpha_s/\pi) + \cdots$ and $\gamma_m(\alpha_s) \equiv \gamma_1(\alpha_s/\pi) + \cdots$ are the QCD β-function and quark mass anomalous dimension: $-\beta_1 = (1/2)(11 - 2n_f/3)$, $\gamma_1 = 2$ for $SU(3)_c \times SU(n_f)$. A QCD spectral sum rule (QSSR) [51,52][5] analysis of the corresponding two-point correlator in the chiral limit ($m_q = 0$):

$$\psi_g(q^2) = i\int d^4x \langle 0|\mathcal{T}\theta^\mu_\mu(x)\theta^\mu_\mu(0)|0\rangle \tag{6.2}$$

from the subtracted and unsubtracted Laplace sum rules:

$$\mathcal{L}_0(\tau) = \int_0^\infty dt e^{t\tau}\frac{1}{\pi}\mathrm{Im}\psi_g(t)$$

$$\mathcal{L}_{-1}(\tau) = -\psi_g(0) + \int_0^\infty \frac{dt}{t} e^{t\tau}\frac{1}{\pi}\mathrm{Im}\psi_g(t) \tag{6.3}$$

leads to the predictions

$$M_\sigma \approx (0.95\text{–}1.10)\ \text{GeV} \quad \text{and} \quad M_G \approx (1.5\text{–}1.6)\ \text{GeV} \tag{6.4}$$

for the masses of the σ/f_0 and scalar gluonium states.

- *σ/f_0 hadronic width from vertex sum rules*

The σ hadronic width can be estimated from the vertex function:

$$V\big[q^2 \equiv (q_1-q_2)^2\big] = \langle \pi|\theta^\mu_\mu|\pi\rangle, \tag{6.5}$$

which obeys a once subtracted dispersion relation [40,41]:

$$V(q^2) = V(0) + q^2\int_{4m_\pi^2}^\infty \frac{dt}{t}\frac{1}{t-q^2-i\epsilon}\frac{1}{\pi}\mathrm{Im}V(t) \tag{6.6}$$

From the low-energy constraints:

$$V(0) = \mathcal{O}(m_\pi^2) \to 0, \quad V'(0) = 1, \tag{6.7}$$

one can derive the low-energy sum rules :

$$\frac{1}{4}\sum_{S\equiv\sigma,\ldots} g_{S\pi\pi}\sqrt{2}f_S = 0, \quad \frac{1}{4}\sum_{S\equiv\sigma,\ldots} g_{S\pi\pi}\frac{\sqrt{2}f_S}{M_S^2} = 1, \tag{6.8}$$

where f_S is the scalar decay constant normalized as

$$\langle 0|4\theta^\mu_\mu|S\rangle = \sqrt{2}f_S M_S^2\,, \tag{6.9}$$

with [41]:

$$f_\sigma \simeq 1\ \text{GeV}, \quad f_{\sigma'} \simeq 0.6\ \text{GeV}, \quad f_G \simeq 0.4\ \text{GeV}, \tag{6.10}$$

for $M_\sigma \simeq 1$ GeV, $M_{\sigma'} \simeq 1.3$ GeV and $M_G \simeq 1.5$ GeV. The first sum rule requires the existence of two resonances, σ/f_0 and its radial excitation σ', coupled strongly to $\pi\pi$.[6] Solving the second sum rule gives, in the chiral limit,

$$|g_{\sigma\pi^+\pi^-}| \simeq |g_{\sigma K^+K^-}| \simeq (4\text{–}5)\ \text{GeV}, \tag{6.11}$$

which suggests an universal coupling of the σ/f_0 to Goldstone boson pairs as confirmed from the $\pi\pi$ and $\bar K K$ scatterings data analysis [22,23]. This result leads to the hadronic width:

$$\Gamma_{\sigma\to\pi\pi} \equiv \frac{|g_{\sigma\pi^+\pi^-}|^2}{16\pi M_\sigma}\left(1-\frac{4m_\pi^2}{M_\sigma^2}\right)^{1/2} \approx 0.7\ \text{GeV}. \tag{6.12}$$

This large width into $\pi\pi$ is a typical OZI-violation expected to be due to large non-perturbative effects in the region below 1 GeV. Its value compares quite well with the width of the so-called on-shell σ/f_0 mass obtained in Ref. [20–22] (see also the next subsection).

- *$\sigma/f_0 \to \gamma\gamma$ width from some low-energy theorems*

We introduce the gauge invariant scalar meson coupling to $\gamma\gamma$ through the interaction Lagrangian and related coupling:

$$\mathcal{L}_{int} = \frac{g_{S\gamma\gamma}}{2}F_{\mu\nu}F^{\mu\nu}\,, \quad \mathcal{P}(0,0) \equiv \tilde g_{S\gamma\gamma} = \left(\frac{2}{e^2}\right) g_{S\gamma\gamma}\,, \tag{6.13}$$

where $F_{\mu\nu}$ is the photon field strength. In momentum space, the corresponding interaction reads[7]

$$\mathcal{L}_{int} = 2 g_{S\gamma\gamma} P_{\mu\nu}(q_1 q_2) \times \epsilon_1^\mu \epsilon_2^\nu, \tag{6.14}$$

where ϵ_i^μ are the photon polarizations. With this normalization, the decay width reads

$$\Gamma = |g_{S\gamma\gamma}|^2 \frac{M_S^3}{8\pi}\left(\frac{1}{2}\right) = \frac{\pi}{4}\alpha^2 M_S^3 |\tilde g_{S\gamma\gamma}|^2, \tag{6.15}$$

where 1/2 is the statistical factor for the two-photon state. One can for instance estimate the $\sigma\gamma\gamma$ coupling by identifying the

[4] For recent reviews on the experimental searches and on the theoretical studies of gluonia, see e.g. Refs. [43–46].

[5] For reviews, see the textbooks in Refs. [53,54] and reviews in Refs. [55,56].

[6] The $G(1600)$ is found to couple weakly to $\pi\pi$ and might be identified with the gluonium state obtained in the lattice quenched approximation (for a recent review of different lattice results, see e.g. [43]).

[7] We use the normalization and structure in [57] for on-shell photons. However, a more general expression is presented in [29] for off-shell photons. We plan to come back to this point in a future publication.

Table 3
Expressions of the weight functions defined in Eq. (5.6) after angular integration in the Euclidian space [$D_{m1} \equiv (P+Q_1)^2+m^2$, $D_{m2} \equiv (P-Q_2)^2+m^2$].

$$
\begin{aligned}
w_1^{PP}(M) &= -\int \frac{d\Omega_1}{2\pi^2}\int \frac{d\Omega_2}{2\pi^2}\,\frac{\pi^2 Q_1 Q_2}{D_{m1}D_{m2}}\,\frac{T_{1E}^{S;PP}(Q_1,Q_2)}{(Q_2^2+M_S^2)[(Q_1+Q_2)^2+M^2]} \\
&= -\frac{2}{3}\frac{\pi^2 Q_1 Q_2}{{Q_2}^2+{M_S}^2}\Big[1+\frac{{Q_2}^2}{2m_l^2}+{Q_2}^2\left({Q_1}^2-{Q_2}^2-M^2\right)\left({Q_1}^2-{Q_2}^2-M^2-4m_l^2\right)I_1^M-\left(2{Q_1}^2-{Q_2}^2-M^2+\frac{{Q_1}^2{Q_2}^2}{2m_l^2}\right)\frac{Rm_1-1}{2m_l^2} \\
&\quad -{Q_2}^2\left(2+\frac{{Q_2}^2}{2m_l^2}\right)\frac{Rm_2-1}{2m_l^2}-\left({Q_1}^2-{Q_2}^2+M^2\right)I_7^M+{Q_2}^2\left(3{Q_1}^2-{Q_2}^2-M^2-4m_l^2+\frac{{Q_1}^2{Q_2}^2}{2m_l^2}\right)\frac{Rm_1-1}{2m_l^2}\,\frac{Rm_2-1}{2m_l^2} \\
&\quad +\left({Q_1}^2+{Q_2}^2+M^2\right)\left(2{Q_1}^2-{Q_2}^2-M^2\right)\frac{Rm_1-1}{2m_l^2}I_7^M-2{Q_2}^2\left({Q_1}^2-M^2\right)\frac{Rm_2-1}{2m_l^2}I_7^M\Big], \\
w_1^{PQ}(M) &= -\int \frac{d\Omega_1}{2\pi^2}\int \frac{d\Omega_2}{2\pi^2}\,\frac{\pi^2 Q_1 Q_2}{D_{m1}D_{m2}}\,\frac{1}{M_S^2}\,\frac{T_{1E}^{S;PQ}(Q_1,Q_2)}{(Q_2^2+M_S^2)[(Q_1+Q_2)^2+M^2]} \\
&= -\frac{1}{3}\frac{\pi^2 Q_1 Q_2}{{M_S}^2\left({Q_2}^2+{M_S}^2\right)}\Big[{Q_1}^2+{Q_2}^2-M^2+2\frac{{Q_1}^2{Q_2}^2}{m_l^2}-4{Q_1}^2{Q_2}^2M^2\left({Q_1}^2-2{Q_2}^2-M^2-4m_l^2\right)I_1^M-{Q_1}^2({Q_1}^2 \\
&\quad -3{Q_2}^2-5M^2+2\frac{{Q_1}^2{Q_2}^2}{m_l^2})\frac{Rm_1-1}{2m_l^2}-4{Q_2}^2\left(2{Q_1}^2+\frac{{Q_1}^2{Q_2}^2}{2m_l^2}\right)\frac{Rm_2-1}{2m_l^2}-\left({Q_1}^2-{Q_2}^2+M^2\right)\left({Q_1}^2-{Q_2}^2-M^2\right)I_7^M \\
&\quad +4{Q_1}^2{Q_2}^2\left(2{Q_1}^2-{Q_2}^2-M^2-4m_l^2+\frac{{Q_1}^2{Q_2}^2}{2m_l^2}\right)\frac{Rm_1-1}{2m_l^2}\frac{Rm_2-1}{2m_l^2}+{Q_1}^2\Big(\left({Q_1}^2-{Q_2}^2\right)^2-4M^2{Q_1}^2-8{Q_2}^2M^2 \\
&\quad -5M^4\Big)\frac{Rm_1-1}{2m_l^2}I_7^M+8M^2{Q_1}^2{Q_2}^2\frac{Rm_2-1}{2m_l^2}I_7^M\Big], \\
w_2^{PP}(M) &= +\int \frac{d\Omega_1}{2\pi^2}\int \frac{d\Omega_2}{2\pi^2}\,\frac{\pi^2 Q_1 Q_2}{D_{m1}D_{m2}}\,\frac{T_{2E}^{S;PP}(Q_1,Q_2)}{[(Q_1+Q_2)^2+M_S^2][(Q_1+Q_2)^2+M^2]} \equiv \frac{\tilde{w}_2^{PP}(M)-\tilde{w}_2^{PP}(M_S)}{M_S^2-M^2}, \\
w_2^{PQ}(M) &= -\int \frac{d\Omega_1}{2\pi^2}\int \frac{d\Omega_2}{2\pi^2}\,\frac{\pi^2 Q_1 Q_2}{D_{m1}D_{m2}}\,\frac{1}{M_S^2}\,\frac{T_{2E}^{S;PQ}(Q_1,Q_2)}{[(Q_1+Q_2)^2+M_S^2][(Q_1+Q_2)^2+M^2]} \equiv \frac{\tilde{w}_2^{PQ}(M)-\tilde{w}_2^{PQ}(M_S)}{M_S^2(M_S^2-M^2)},
\end{aligned}
$$

with

$$
\begin{aligned}
\tilde{w}_2^{PP}(M) &= \frac{2}{3}\pi^2 Q_1 Q_2\Big(2M^2\left({Q_1}^2{Q_2}^2+m_l^2{Q_1}^2+m_l^2{Q_2}^2+m_l^2M^2\right)I_1^M+\frac{{Q_1}^2}{2}\frac{Rm_1-1}{2m_l^2}+\frac{{Q_2}^2}{2}\frac{Rm_2-1}{2m_l^2}+M^2I_7^M \\
&\quad -\left({Q_1}^2{Q_2}^2+2m_l^2M^2\right)\frac{Rm_1-1}{2m_l^2}\frac{Rm_2-1}{2m_l^2}-\frac{{Q_1}^2}{2}\left({Q_1}^2-{Q_2}^2+3M^2\right)\frac{Rm_1-1}{2m_l^2}I_7^M-\frac{{Q_2}^2}{2}\left({Q_2}^2-{Q_1}^2+3M^2\right)\frac{Rm_2-1}{2m_l^2}I_7^M\Big), \\
\tilde{w}_2^{PQ}(M) &= -\frac{1}{3}\pi^2 Q_1 Q_2\Big[-M^2+2M^2{Q_1}^2{Q_2}^2({Q_1}^2+{Q_2}^2+4m_l^2)I_1^M+\frac{{Q_1}^2}{2}\left({Q_1}^2+3{Q_2}^2+M^2\right)\frac{Rm_1-1}{2m_l^2} \\
&\quad +\frac{{Q_2}^2}{2}({Q_2}^2+3{Q_1}^2+M^2)\frac{Rm_2-1}{2m_l^2}+M^2({Q_1}^2+{Q_2}^2+M^2)I_7^M-2{Q_1}^2{Q_2}^2\left({Q_1}^2+{Q_2}^2+4m_l^2\right)\frac{Rm_1-1}{2m_l^2}\frac{Rm_2-1}{2m_l^2}-\frac{{Q_1}^2}{2} \\
&\quad \times({Q_1}^4-{Q_2}^4+2M^2{Q_1}^2+4M^2{Q_2}^2+M^4)\frac{Rm_1-1}{2m_l^2}I_7^M-\frac{{Q_2}^2}{2}({Q_2}^4-{Q_1}^4+2M^2{Q_2}^2+4M^2{Q_1}^2+M^4)\frac{Rm_2-1}{2m_l^2}I_7^M\Big],
\end{aligned}
$$

and

$$
I_1^M=\frac{1}{m_l^2{Q_1}^2{Q_2}^2}\ln[1-Z^M_{Q_1Q_2}Z^{m_l}_{PQ_1}Z^{m_l}_{PQ_2}],\qquad I_7^M=\frac{Z^M_{Q_1Q_2}}{Q_1Q_2},\qquad R_{mi}\equiv\sqrt{1+\frac{4m_l^2}{Q_i^2}},\qquad Z^{m_l}_{PQ_i}=\frac{Q_i}{2P}(1-R_{mi}),
$$

$$
(Z^{m_l}_{PQ_i})^2=\frac{Q_i}{P}Z^{m_l}_{PQ_i}-1,\qquad Z^{m_l}_{PQ_1}Z^{m_l}_{PQ_2}=-\frac{Q_1Q_2}{4m_l^2}(R_{m1}-1)((R_{m2}-1)),\qquad Z^M_{KL}=\frac{K^2+L^2+M^2-\sqrt{(K^2+L^2+M^2)^2-4K^2L^2}}{2KL},
$$

Euler–Heisenberg Lagrangian derived from $gg\to\gamma\gamma$ via a quark constituent loop with the interaction Lagrangian in Eq. (6.13). In this way, one deduces the constraint[8]:

$$
g_{S\gamma\gamma}\simeq\frac{\alpha}{60}\sqrt{2}f_S M_S^2\left(\frac{\pi}{-\beta_1}\right)\sum_{u,d,s}Q_q^2/M_q^4, \tag{6.16}
$$

where Q_q is the quark charge in units of e; $M_{u,d}\approx M_\rho/2$ and $M_\phi\approx M_\phi/2$ are constituent quark masses. Then, one obtains:

$$
g_{\sigma\gamma\gamma}\approx g_{\sigma'\gamma\gamma}\approx g_{G\gamma\gamma}\approx(0.4\text{–}0.7)\alpha\ \text{GeV}^{-1}, \tag{6.17}
$$

which leads, for $M_\sigma\simeq 1$ GeV, to the $\gamma\gamma$ width:

$$
\Gamma_{\sigma\to\gamma\gamma}\simeq(0.2\text{–}0.6)\ \text{keV}. \tag{6.18}
$$

A consistency check of the previous result can be obtained from the trace anomaly $\langle 0|\theta^\mu_\mu|\gamma\gamma\rangle$ by matching the k^2 dependence of its two sides which leads to [58–61]:

$$
\frac{1}{4}\sum_{S=\sigma\cdots}g_{S\gamma\gamma}\sqrt{2}f_S=\frac{\alpha R}{3\pi}, \tag{6.19}
$$

where $R\equiv 3\sum Q_q^2$.

7. $\sigma/f_0(500)$ meson from $\pi\pi$ and $\gamma\gamma$ scattering

The mass and the width of a broad resonance like the $\sigma/f_0(500)$ state in general turn out to be rather ambiguous quantities. A non ambiguous definition is provided by the location of the pole of the S-matrix amplitude on the second Riemann sheet [62]. The difficulty then lies in relating this pole in the complex domain to the description, for instance in the form of a Breit–Wigner function, of the data on the positive real axis. This issue has been quite extensively discussed in the context of the line-shapes of the electroweak gauge and scalar bosons[9] [63–69].

[8] This sum rule has been originally used by [39] in the case of a charm quark loop for estimating the $J/\psi\to\gamma\sigma$ radiative decay.

[9] The issue was mainly centred around the necessity to define gauge-invariant observables and to correctly account for threshold effects.

In this section, the information on the f_0/σ resonance that can be obtained from data on $\pi\pi$ scattering or on $\gamma\gamma \to \pi^0\pi^0$, $\pi^+\pi^-$ are reviewed. We then end this section by specifying how the contribution to HLbL from a broad object like the $\sigma/f_0(500)$ can be described by the formalism that we have set up in Section 3.

- *σ/f_0 mass and width in the complex plane*

The mass and width of the σ/f_0 meson play an important rôle in the present analysis. Their precise determinations in the complex plane from $\gamma\gamma \to \pi^0\pi^0$, $\pi^+\pi^-$ scattering data in Ref. [20] (one resonance $\oplus$ one channel) and in Refs. [21,22] (two resonances $\oplus$ two channels and adding the K_{e4} data), lead to the complex pole:

$$M_\sigma^c \equiv M_\sigma - i\Gamma_\sigma/2, \\ \simeq \big[452(12) - \mathrm{i}260(15)\big]\ \mathrm{MeV}, \tag{7.1}$$

which agrees with some other estimates from $\pi\pi$ scattering data for one channel [70–72]. Using the model of [19] for separating the direct and rescattering contributions, one obtains from $\gamma\gamma \to \pi\pi$ scatterings data [20–22]:

$$\Gamma_\sigma^{\gamma\gamma}|^{dir} \simeq (0.16 \pm 0.04)\ \mathrm{keV}, \\ \Gamma_\sigma^{\gamma\gamma}|^{resc} \simeq (1.89 \pm 0.81)\ \mathrm{keV}, \\ \Gamma_\sigma^{\gamma\gamma}|^{tot} \simeq (3.08 \pm 0.82)\ \mathrm{keV}, \tag{7.2}$$

corresponding respectively to the *direct, rescattering* contributions and *their total sum*. The rescattering contribution includes the ones of the Born term, the vector and axial-vector mesons in the t-channel and the $I = 2$ mesons.

- *σ/f_0 Breit–Wigner on-shell mass and widths*

However, an extrapolation of the previous result obtained in the complex plane to the real axis is not straightforward. Then, in the Breit–Wigner analysis for approximately reproducing the data, one may either introduce the *on-shell mass and width* defined in [68] for the Z-bozon and used [20,22,43] within the model of [19]:

$$\mathrm{Re}\,\mathcal{D}[(M_\sigma^{\mathrm{os}})^2] = 0 \implies M_\sigma^{\mathrm{os}} \approx 0.92\ \mathrm{GeV}\,. \tag{7.3}$$

It corresponds to the *on-shell hadronic width* evaluated at $s = (M_\sigma^{\mathrm{os}})^2$:

$$M_\sigma^{\mathrm{os}}\Gamma_\sigma^{\pi\pi}|_{os} \simeq \frac{\mathrm{Im}\,\mathcal{D}}{-\mathrm{Re}\,\mathcal{D}'} \implies \Gamma_\sigma^{\pi\pi}|_{os} \approx 1.04\ \mathrm{GeV}, \tag{7.4}$$

where $\mathcal{D}$ is the inverse propagator and $\mathcal{D}'$ its derivative. The corresponding $\gamma\gamma$ width can be extracted by evaluating Eq. (7.2) at the on-shell mass and gives by including the $f_0(980)$ in the fit analysis [22]:

$$\Gamma_\sigma^{\gamma\gamma}|_{os} \simeq (1.2 \pm 0.3)\ \mathrm{keV}. \tag{7.5}$$

A more recent fit of the data using the Breit–Wigner parametrization leads to [43]:

$$M_\sigma \simeq 1000(100)\ \mathrm{MeV}, \qquad \Gamma_\sigma^{\pi\pi} \simeq 700(70)\ \mathrm{MeV}\,, \tag{7.6}$$

which are consistent with the above results, and with the sum rules results in Eq. (6.4). An earlier fit using K-matrix leads to the value [73]:

$$M_\sigma = 910 - 350\ \mathrm{i}\ \mathrm{MeV}\,, \tag{7.7}$$

quoted without errors.

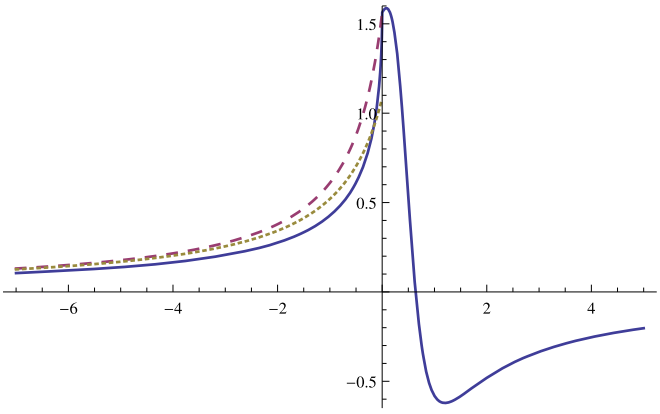

Fig. 6. The function $\widetilde{BW}(s; M_{\mathrm{BW}}, \Gamma_{\mathrm{BW}})$ (solid line) for $M_{\mathrm{BW}} = 0.8$ GeV and $\Gamma_{\mathrm{BW}} = 0.7$ GeV, as a function of s (in GeV^2), compared, for negative values of s, to the function $-1/(s - M_{\mathrm{BW}}^2)$ (dashed line), for the same value of M_{BW}, and to the function $-1/(s - M_{\mathrm{eff}}^2)$ (dotted line), with $M_{\mathrm{eff}} = 1.2 M_{\mathrm{BW}}$, which gives a better description in the region around $s \sim (0.5\ \mathrm{GeV})^2$.

- *Breit–Wigner function in the space-like domain*

Let us assume that the data on the real positive axis are described in terms of a Breit–Wigner function $BW(s; M_{\mathrm{BW}}, \Gamma_{\mathrm{BW}})$ for some values of the Breit–Wigner mass M_{BW} and width Γ_{BW}. In order to extend this function on the whole real s-axis without introducing any singularity besides the cut along the positive real axis, one considers the function [76,77]:

$$\widetilde{BW}(s; M_{\mathrm{BW}}, \Gamma_{\mathrm{BW}}) = \frac{1}{\pi}\int_0^\infty dx\, \frac{\mathrm{Im}\,BW(s; M_{\mathrm{BW}}, \Gamma_{\mathrm{BW}})}{x - s - i\epsilon}. \tag{7.8}$$

For:

$$BW(s; M_{\mathrm{BW}}, \Gamma_{\mathrm{BW}}) = \frac{1}{s - M_{\mathrm{BW}}^2 - i\sqrt{s}\,\Gamma_{\mathrm{BW}}}, \tag{7.9}$$

one finds $\widetilde{BW}(s; M_{\mathrm{BW}}, \Gamma_{\mathrm{BW}}) = BW(s; M_{\mathrm{BW}}, \Gamma_{\mathrm{BW}})$ for $s > 0$, and for $s = -Q^2 < 0$:

$$\widetilde{BW}(-Q^2; M_{\mathrm{BW}}, \Gamma_{\mathrm{BW}}) = \frac{-1}{Q^2 + M_{\mathrm{BW}}^2 + \sqrt{Q^2}\,\Gamma_{\mathrm{BW}}}. \tag{7.10}$$

In the narrow-width approximation, this reduces to the usual Euclidian version of the Feynman propagator. But the latter represents a good approximation even when the width becomes sizeable. This is illustrated in Fig. 6 for the case $\Gamma_{\mathrm{BW}} \sim M_{\mathrm{BW}}$. One can also represent the function $\widetilde{BW}(s; M_{\mathrm{BW}}, \Gamma_{\mathrm{BW}})$ in the space-like region by a propagator term $-1/(s - M_{\mathrm{eff}}^2)$, with M_{eff} adjusted, for instance, to give a more accurate description of $\widetilde{BW}(s; M_{\mathrm{BW}}, \Gamma_{\mathrm{BW}})$ in the region of values of Q^2 that matters most from the point of view of the weight functions displayed in Figs. 3 and 5. Given the large uncertainties in the mass of the $\sigma/f_0(500)$, such refinements will actually not be necessary.

8. Adopted values of the $\sigma/f_0(500)$ mass and widths

- *$\sigma/f_0(500)$ mass and hadronic width*

Assuming that the relative errors in the fitting procedure of Ref. [73] are the same as the ones in Ref. [43] and taking the range of values spanned by the three different determinations including the sum rules results in Eq. (6.4), we adopt the values:

$$M_\sigma \simeq (960 \pm 96),\ \mathrm{MeV} \qquad \Gamma_\sigma^{\pi\pi} \simeq (700 \pm 70)\ \mathrm{MeV}, \tag{8.1}$$

which implicitly includes in its definition the large hadronic width of the σ-meson. One should notice that the three predictions for the widths agree each other and we have assumed a guessed error of 10%.

We compare the previous values with the range given by PDG [25] for a Breit–Wigner (BW) mass and hadronic width (in units of MeV):

$$M_\sigma \simeq (400-550)\,, \qquad \Gamma_\sigma^{\pi\pi} \simeq (400-700)\,, \tag{8.2}$$

where we notice that our predictions for the BW mass are slightly higher.

- $\sigma/f_0(500) \to \gamma\gamma$ *width*

For the $\gamma\gamma$ width, PDG does not provide any estimated range of values. Among the different estimates proposed in the literature which often refer to the *total* $\gamma\gamma$*-width* of the σ in the complex plane, we consider the most recent determinations in Eq. (7.2) from [22] and the ones in Refs. [74,75]. Averaging these results with the one in Eq. (7.5) from [22], we obtain:

$$\Gamma_\sigma^{\gamma\gamma}|^{tot}_{mean} \simeq (1.82 \pm 0.32)\ \text{keV} \tag{8.3}$$

where we have doubled the error for a conservative result. This *total* $\gamma\gamma$*-width* is larger than expected from a pure glueball state [40,41] indicating the complex dynamics for extracting the width from the data. The corresponding coupling is:

$$\tilde{g}_{\sigma\gamma\gamma} \equiv \left(\frac{2}{e^2}\right) g_{\sigma\gamma\gamma} \simeq (0.24 \pm 0.02)\ \text{GeV}^{-1}. \tag{8.4}$$

9. $\gamma\gamma$ widths of other scalar mesons

- $f_0(1370)$ *and* $G \equiv f_0(1500)$ *scalar mesons*

Considering the $f_0(1370)$ and $G \equiv f_0(1500)$ as gluonium-like scalar mesons [40,41], their $\gamma\gamma$ couplings are expected to be given by the sum rule in Eq. (6.17). Then, we take approximately these values to be:

$$\tilde{g}_{\sigma'\gamma\gamma} \approx \tilde{g}_{G\gamma\gamma} \simeq (0.09 \pm 0.02)\ \text{GeV}^{-1}. \tag{9.1}$$

- $f_0(990)$ *scalar meson*

The true nature of the $f_0(990)$ is still unclear. However, the large ratio of its coupling $|g_{fK^+K^-}/g_{f\pi^+\pi^-}| \simeq (1.7\text{–}2.6)$ from $\pi\pi$, $\bar{K}K$ scatterings and J/ψ-decay data [22,23] does not favour its $\bar{q}q$ interpretation but instead indicates some gluon or/and four-quark components. A fit of the $\gamma\gamma$ scattering data leads to the *direct width* [22]:

$$\Gamma_{f_0}^{\gamma\gamma}|^{dir} \simeq 0.28(1)\ \text{keV}, \tag{9.2}$$

which has the same value as the one quoted by PDG [25]:

$$\Gamma_{f_0}^{\gamma\gamma}|_{PDG} = (0.29 \pm 0.07)\ \text{keV}, \tag{9.3}$$

from which we deduce the coupling from the *direct width*:

$$\tilde{g}_{f_0\gamma\gamma} \simeq (0.09 \pm 0.02)\ \text{GeV}^{-1}. \tag{9.4}$$

One can notice that the *rescattering* contribution is large and acts with a destructive interference [22],

$$\Gamma_{f_0}^{\gamma\gamma}|^{resc} \simeq (0.85 \pm 0.05)\ \text{keV}. \tag{9.5}$$

The "sum" of the rescattering and direct contributions leads to the $\gamma\gamma$ *total width*

$$\Gamma_{f_0}^{\gamma\gamma}|^{tot} \simeq (0.16 \pm 0.01)\ \text{keV}, \tag{9.6}$$

which is smaller than the direct contribution in Eq. (9.3). One can consider that the value of the $f_0 \to \gamma\gamma$ width is conservatively given by the range spanned by the direct and total widths

$$\Gamma_{f_0}^{\gamma\gamma} = (0.22 \pm 0.07)\ \text{keV} \implies \tilde{g}_{f_0\gamma\gamma} \simeq (0.07 \pm 0.02)\ \text{GeV}^{-1}, \tag{9.7}$$

which is close to the one given in Eq. (9.3) by PDG. Then, in our analysis, we shall use the PDG value, which gives:

$$\tilde{g}_{f_0\gamma\gamma} \simeq (0.09 \pm 0.01)\ \text{GeV}^{-1}. \tag{9.8}$$

- $a_0(980)$ *scalar meson*

We shall use the value quoted by PDG [25]:

$$\Gamma_{a_0}^{\gamma\gamma}\left(\frac{\Gamma_{a_0}^{\eta\pi}}{\Gamma_{a_0}^{tot}}\right) = \left(0.21^{+0.07}_{-0.04}\right)\ \text{keV}, \tag{9.9}$$

where again the rescattering contribution is important [80]. We deduce:

$$\tilde{g}_{a_0\gamma\gamma} \simeq \left(0.09^{+0.02}_{-0.01}\right)\ \text{GeV}^{-1}, \tag{9.10}$$

where we have used : $\Gamma_{a_0}^{\eta\pi}/\Gamma_{a_0}^{tot} \simeq 0.82$ [25].

- $a_0(1450)$ *scalar meson*

The origin of the $\gamma\gamma$ width from Belle data on $\gamma\gamma \to \pi^0\eta$ as quoted by the PDG [25] is quite uncertain. Its value is:

$$\Gamma_{a_0}^{\gamma\gamma}\left(\frac{\Gamma_{a_0}^{\eta\pi}}{\Gamma_{a_0}^{tot}}\right) \simeq \left(0.43^{+1.07}_{-0.26}\right)\ \text{keV}. \tag{9.11}$$

Using, $\Gamma_{a_0}^{\eta\pi}/\Gamma_{a_0}^{tot} \simeq 0.093 \pm 0.020$ and $M_{a_0} = 1474$ MeV, one deduces:

$$\tilde{g}_{a_0\gamma\gamma} \simeq (0.26 \pm 0.14)\ \text{GeV}^{-1}\,. \tag{9.12}$$

10. $a_\mu^{lbl}|_S$ and comparison with some other evaluations

The scalar exchange contribution to the muon anomalous magnetic moment is given by Eq. (5.4). The integrals $\mathcal{I}_p$, $\mathcal{I}_{pq}$, $\mathcal{I}_q$ have been evaluated numerically, and their values are given in Table 4 versus the value of the scalar meson mass. Our results in Table 4, which are shown for different values of κ_S, are expected to take into account all S-waves contributions (direct $\oplus$ rescattering) as we have used the *total* $\gamma\gamma$ widths for each meson. Before going over to the comparison of our results with some of those already available in the literature, let us make a few comments about the results shown in Table 4:

- As discussed at the end of Section 4, an analysis based only on the leading short-distance behaviour of the vertex function $\Gamma^S_{\mu\nu}$ and on the VMD representation of the form factors does not properly account for the decay of pure isovector scalar states into two photons, whereas the analysis of Ref. [29] leads to the choice $\kappa_S = 1$ in this case. Due to the possible mixing of the isoscalar mesons with gluonium states, the corresponding value of κ_S cannot be fixed without further knowledge on the matrix elements in

Table 4
Scalar mesons contributions to $a_\mu^{lbl}|_S$ versus their masses. The parameter κ_S is defined in Eq. (4.6). The errors in the sum have been added quadratically. The $\mathcal{I}_s$ integrals with $s \equiv p, pq, q$ are multiplied by 10^2. We use $M_\sigma = (960 \pm 96)$ MeV (see text) and $M_V \equiv M_\rho = 775$ MeV. For the other scalars, the masses are given (in MeV) between parentheses. The errrors on $\mathcal{I}_{p,\dots}$ are due to the meson masses. The errors have been added quadratically.

Scalar	$\tilde{g}_{S\gamma\gamma}$ [GeV^{-1}]	$-\mathcal{I}_p$ [GeV^2]	$\mathcal{I}_{pq}$ [GeV^2]	$\mathcal{I}_q$ [GeV^2]	$a_\mu^{lbl}\|_S \times 10^{11}$	
					$\kappa_S = 0$	$\kappa_S = +1$
$f_0/\sigma(960)$	(0.24 ± 0.02)	$\left(4.35^{-0.66}_{+0.84}\right)$	$\left(1.17^{-0.27}_{+0.39}\right)$	$\left(2.75^{-0.96}_{+1.63}\right)$	$-\left(3.14^{-0.72}_{+0.84}\right)$	$-\left(0.31^{+0.41}_{-0.82}\right)$
$a_0(980)$	(0.09 ± 0.02)	4.20	1.11	2.51	$-(0.43 \pm 0.14)$	$-(0.06 \pm 0.03)$
$f_0(990)$	(0.09 ± 0.01)	4.12	1.08	2.40	$-(0.42 \pm 0.09)$	$-(0.07 \pm 0.02)$
$f_0(1350)$	(0.09 ± 0.02)	2.38	0.44	0.59	$-(0.24 \pm 0.11)$	$-(0.14 \pm 0.06)$
$a_0(1474)$	$\left(0.19^{+0.21}_{-0.08}\right)$	2.03	0.34	0.39	$-\left(0.92^{+3.15}_{-0.61}\right)$	$-\left(0.59^{+2.02}_{-0.39}\right)$
$f_0(1504)$	(0.09 ± 0.02)	1.96	0.32	0.36	$-(0.20 \pm 0.09)$	$-(0.13 \pm 0.06)$
Total					$-\left(5.35^{+3.27}_{-0.92}\right)$	$-\left(1.3^{+2.06}_{-0.91}\right)$

Eq. (4.3), and will in general even be different for each scalar meson. In Table 4 we have considered two values of κ_S: $\kappa_S = 0$, i.e. no contribution from the form factor $\mathcal{Q}(q_1, q_2)$, and $\kappa_S = 1$, which follows from the analysis of Ref. [29].

• One can notice that the contributions from the $\sigma/f_0(500)$ to a_μ^{lbl} dominate over the other scalar contributions, independently of the value of κ_S. This dominance of the σ contribution over the other scalar mesons can be understood, on the one hand, from the behaviour of the weight functions defined in Table 3 and shown in Figs. 3, 4 and 5 versus Q_1^2 and Q_2^2, which are more weighted, like in the case of the pion exchange [28], for the mesons of lower masses, and, on the other hand, by the fact that the $\gamma\gamma$ couplings of higher states are much smaller than the one of the σ.

• The contributions of the higher-mass states $f_0(1370)$, $a_0(1450)$ and $f_0(1500)$ are not suppressed as compared to the lighter states $a_0(980)$ and $f_0(990)$ as could naively be expected from a simple scaling argument of the masses. Another important parameter here is the two-photon width. The coupling of the heavier scalars to a photon pair turns out to be rather strong as compared to the light scalars.

• If we only consider the contribution from the Lorentz structure $\mathcal{P}_{\mu\nu}$ to the $\sigma\gamma\gamma$ form factor in Eq. (3.2), like often done in the current literature, one obtains [case $\mathcal{Q}(0,0) = 0$ in Table 4]:

$$a_\mu^{lbl}|_\sigma = -\left(5.35^{+3.27}_{-0.92}\right) \times 10^{-11}, \tag{10.1}$$

where the σ contribution is comparable in size and sign with the resuls obtained by other authors [12,15] [the value given in Ref. [81] is the same as in Ref. [12], but with the uncertainty scaled to 100%], and with the one using $\pi\pi$ rescattering analysis [17] quoted in Table 5, with which some connection can be established from the methodological point of view.

This brings us to a more direct comparison with the results obtained by the authors of Ref. [16] on the one hand, and of Refs. [17, 18] on the other hand.

• The authors of Ref. [16] consider the contribution to HLbL coming from the scalar mesons $f_0(990)$, $a_0(980)$ and $f_0(1370)$ in the same NWA as considered here. They start from a different decomposition of the vertex function $\Gamma^S_{\mu\nu}$:

$$\Gamma^S_{\mu\nu} = \mathcal{F}_{TT} T_{\mu\nu} + \mathcal{F}_{LL} L_{\mu\nu}, \tag{10.2}$$

which describes the production of a scalar meson, for instance in $e^+e^- \to e^+e^- S$ $(\to e^+e^-\pi\pi)$, through either two transverse or two longitudinal photons [78]. The link with the decomposition in Eq. (3.1) is given by:

$$\begin{aligned}\mathcal{F}_{TT}(q_1, q_2) &= -(q_1 \cdot q_2)\mathcal{P}(q_1, q_2) - q_1^2 q_2^2 \mathcal{Q}(q_1, q_2),\\ \mathcal{F}_{LL}(q_1, q_2) &= -(q_1 \cdot q_2)\left[\mathcal{P}(q_1, q_2) + (q_1 \cdot q_2)\mathcal{Q}(q_1, q_2)\right].\end{aligned} \tag{10.3}$$

In their analysis, they assume that the contribution from the longitudinal part $\mathcal{F}_{LL}(q_1, q_2)$ is suppressed [as compared to the one from $\mathcal{F}_{TT}(q_1, q_2)$] and thus they do not consider it. Moreover, they use, for the transverse form factor, a monopole representation, which is reproduced by the VMD representation used here when $B = 0$, i.e. $\kappa_S = 0$, a choice which then consistently also entails that $\mathcal{Q}^{\text{VMD}}(q_1, q_2) = 0$ (see Eq. (4.5)). As shown by the results in Table 4, the contribution from the form factor $\mathcal{Q}(q_1, q_2)$ is in general substantial.

• In Refs. [17,18], the $\pi\pi$ rescattering effects to HLbL are considered, with $\gamma^*\gamma^* \to \pi\pi$ helicity partial waves $h_{J;\lambda_1\lambda_2}$ [λ_i denote the photon helicities] constructed dispersively, using $\pi\pi$ phase shifts derived from the inverse amplitude method. The $I = 0$ part of this calculation, which gives:

$$a_{\mu;\,J=0;I=0}^{\pi\pi;\,\pi-\text{pole LHC}} = -9 \cdot 10^{-11} \tag{10.4}$$

with a precision of 10%, can be interpreted as the contribution from the $\sigma/f_0(500)$ meson. The mention "π − pole LHC" means that the left-hand cut is provided by the Born term alone, i.e. single-pion exchange in the t channel. Instead of $\Gamma^S_{\mu\nu}$, the starting point is the matrix element:

$$\int d^4x\, e^{iq_1\cdot x} \langle \Omega | T\{j_\mu(x) j_\nu(0)\} | \pi^a(p_1)\pi^b(p_2)\rangle, \tag{10.5}$$

where either $a = b = 0$, or $a = +$, $b = -$. These matrix element can be decomposed in terms of five independent invariant functions A_i in the following way (see e.g. Ref. [79]):

$$-A_1 P_{\mu\nu}(q_1, q_2) - A_2 Q_{\mu\nu}(q_1, q_2) + \sum_{i=3,4,5} A_i T^i_{\mu\nu}(q_1, q_2), \tag{10.6}$$

where $p_1 + p_2 = q_1 + q_2$. The expressions of the remaining tensors $T^i_{\mu\nu}(q_1, q_2)$ for $i = 3, 4, 5$ are not needed here, and can be found in Ref. [79]. What matters is that, upon performing a partial wave decomposition, only A_1 and A_2 receive contributions from the S wave. In the NWA, the vertex function $\Gamma^S_{\mu\nu}(q_1, q_2)$ arises as the residue of the pole as $s \equiv (q_1 + q_2)^2 \to M_S^2$, the correspondence being:

$$h_{0,++}(s) \to -\frac{1}{4}\mathcal{F}_{TT},\ h_{0,00}(s) \to -\frac{1}{4}\frac{\sqrt{q_1^2}\sqrt{q_2^2}}{(q_1 \cdot q_2)}\mathcal{F}_{LL}. \tag{10.7}$$

In addition, the Born term in the $\pi^+\pi^-$ channel only contributes to A_1 and to A_4, which in turn has no $J = 0$ component, but not to A_2. There is therefore a relation between the Born term contributions to $h_{0,++}$ and to $h_{0,00}$, which effectively amounts to the condition $\mathcal{Q}(q_1, q_2) = 0$, i.e. $\kappa_S = 0$. The result we obtain for this

Table 5
Different estimates of the scalar meson contributions via LbL scattering at lowest order (LO). We use $\Gamma_\sigma^{\gamma\gamma} = 1.62(42)$ keV in Eq. (8.4).

Scalar	$a_\mu^{lbl}\vert_S \times 10^{11}$	Refs.
This work		
$\sigma(960 \pm 96)$	$-\left(3.14^{+0.84}_{-0.72}\right) \leq \ldots \leq -\left(0.31^{+0.41}_{-0.82}\right)$	This work
$\sum_{a_0, f_0, \ldots}$	$-\left(2.21^{+3.16}_{-0.65}\right) \leq \ldots \leq -\left(0.99^{+2.02}_{-0.40}\right)$	–
Total sum	$-\left(5.35^{+3.27}_{-0.92}\right) \leq \ldots \leq -\left(1.3^{+2.06}_{-0.91}\right)$	–
Final result	$-(4.51 \pm 4.12)$	This work
Others		
$\sigma(620)$	$-(6.8 \pm 2.0)$	ENJL [12]
$\sigma(620)$	$-(6.8 \pm 6.8)$	ENJL [81]
$\sigma(400-600)$	$-(36 \sim 7)$	[15]
$\pi\pi$-rescattering	$-(7.8 \pm 0.5)$	π pole [17]

Table 6
Recent determinations of the LO hadron vacuum polarization (HVP) in units of 10^{-11} from the data compared with some other models and lattice results. The tentative theoretical average is more weighted by the most precise determinations in [84,85]. The weighted averaged error is informative. Instead, one may use the one from the precise determinations which is about twice the averaged error.

Values	Refs.
Data	
6880.7±41.4	[82]
6931±34	[83]
6933±25	[84]
6922.4 ± 18.1	*Data average*
Models ⊕ Lattice data	
6932±25	[85]
6818±31	[86]
6344±354	[87]
Lattice	
6740±277	[88]
6670±134.2	[89]
7110±188.6	[90]
6540±388	[91]
7154±187	[92]
6830±180	[93]
Tentative theoretical average	
6904.02±13.06	

Table 7
Comparison of the different determinations of the pseudoscalar meson contributions in units of 10^{-11}. We have taken the mean of the asymmetric errors in the average which is about 0.8 the one of the most precise error.

Values	Approaches	Refs
83.0±12.0	Vector Meson Dominance	[28]
$84.0^{+8.7}_{-8.1}$	Vector Meson Dominance	[94]
$89.9^{+9.7}_{-8.9}$	Lowest Meson Dominance ⊕ Vector	[94]
$84.7^{+5.3}_{-1.8}$	Resonance Chiral Theory	[95]
85.0 ± 3.6		*Average*

value (see Table 4) is somewhat higher than the number quoted in Eq. (10.4), but this difference can possibly be understood by the absence of a more complete description of the left-hand cut in the analysis of Refs. [17,18].

11. Present experimental and theoretical status

We show in Table 6 the different estimates of a_μ^{hvp}, where one may amazingly notice that the mean of the two recent phenomenological determinations [83] and [84] coïncides with the one obtained in [85] within a theoretical model. Using our new estimate of the scalar meson contributions to the Light-by-Light scattering to a_μ, we show in Table 8 the present experimental and theoretical status on the determinations of a_μ.

Table 8
Comparison of the experimental measurement and theoretical determinations of a_μ within the Standard Model (SM) in units of 10^{-11}. For HVP at LO, we take the tentative theoretical average obtained in Table 6. For the pseudoscalars contributions to HLbL, we take the mean of the ones in Table 7. For the scalars, we take the mean of the errors quoted in the final result of this work in Table 5. The total errors of the sum in the present Table have been added quadratically.

Determinations	Values	Refs
Experiment	11 659 2091.0±63.0	[96]
Theory		
QED at 5 loops	11 658 4718.85±0.36	[97,98]
Electroweak at 2 loops	$+(154.0 \pm 1.0)$	[99,100]
HVP		
LO	$+(6904.02 \pm 13.06)$	Average
NLO	$-(99.34 \pm 0.91)$	[82,101]
N2LO	$+(12.26 \pm 0.12)$	[82]
Total HVP	$+(6816.94 \pm 13.09)$	
HLbL at LO		
Pseudoscalars	$+(85.0 \pm 2.8)$	Average
Scalars	$-(4.51 \pm 4.12)$	This work
Axial-vector	$+(7.5 \pm 2.7)$	[16,82]
Tensor	$+(1.1 \pm 0.1)$	[16]
Total HLbL	$+(88.0 \pm 5.7)$	
$a_\mu^{\rm SM}$	11 659 1778.9 ± 14.3	This work
$a_\mu^{\rm exp} - a_\mu^{\rm SM}$	$+(312.1 \pm 64.6)$	This work

12. Conclusions

We have systematically studied the light scalar meson contributions to the anomalous magnetic moment of the muon a_μ from hadronic light-by-light scattering (HLbL). Our analysis also includes the somewhat heavier states, which however have couplings to two photons at least as strong as those of the $a_0(980)$ and the $f_0(990)$. Our results are summarized in Table 4 and compared with some other determinations in Table 5. We conclude that the HLbL contribution from the scalars is dominated by the σ/f_0 one, which one may understand from the Q^2-behaviour of the weight functions entering into the analysis, and which are plotted in Figs. 3 to 5. Moreover, the uncertainties on the parametrisation of the form factors induce large errors in the results, which might be improved from a better control of these observables. In particular, our analysis draws the attention to the potentially important contribution from the second structure $\mathcal{Q}_{\mu\nu}$ in the decomposition of the vertex function in Eq. (3.1), which could even lead to a change of sign in $a_\mu^{lbl}\vert_\sigma$. For the isovector states, an estimate of its size could be obtained from the analysis of Ref. [29]. For the isoscalar states, mixing with glueball states and/or with $\bar{s}s$ states can lead to important contributions from the whole set of matrix elements in Eq. (4.3). Knowledge of these matrix elements can possibly be obtained, for instance, either from phenomenology or from QCD spectral sum rules. We leave this matter for a future research. For a conservative result, we consider as a (provisional) *final result* the range of values spanned by the two possible values from 0 to 1 of $\mathcal{Q}(0,0)/(M_S^2 \tilde{g}_{S\gamma\gamma})$ obtained in Table 4, which we compare in Table 5 with some other determinations. Finally, we present in Table 8 a new comparison of the data with theoretical predictions including our new results. The theoretical errors from HLbL are dominated by the ones due to the scalar meson contributions. Moreover, some other scalar meson contributions to a_μ from radiative decays of vector mesons and virtual exchange have also

been considered in [102]. We plan to improve these results in a future work.

Acknowledgements

S. Narison wishes to thank Wolfgang Ochs for some useful correspondences, U. Gastaldi for several discussions on the scalar mesons, and the ICTP-Trieste for a partial financial support. M. Knecht wishes to thank P. Sanchez-Puertas for useful remarks on the manuscript. The work of M.K. and S.N. has been carried out thanks to the support of the OCEVU Labex (ANR-11-LABX-0060) and the A*MIDEX project (ANR-11-IDEX-0001-02) funded by the "Investissements d'Avenir" French government program managed by the ANR.

References

[1] B.C. Odom, D. Hanneke, B. D'Urso, G. Gabrielse, Phys. Rev. Lett. 97 (2006) 030801;
B.C. Odom, D. Hanneke, B. D'Urso, G. Gabrielse, Phys. Rev. Lett. 99 (2007) 039902 (Erratum).
[2] D. Hanneke, S. Fogwell, G. Gabrielse, Phys. Rev. Lett. 100 (2008) 120801.
[3] G.W. Bennett, et al., Muon $g-2$ Collaboration, Phys. Rev. D 73 (2006) 072003.
[4] R.M. Carey, et al., Fermilab. Proposal 0989, The New $g-2$ experiment (2009).
[5] B. Lee Roberts, Chin. Phys. C 34 (2010) 741.
[6] T. Gorringe, Muon $g-2$ Collaboration, EPJ Web Conf. 179 (2018) 01004.
[7] T. Mibe, J-PARC $g-2$ Collaboration, Chin. Phys. C 34 (2010) 745.
[8] R. Bouchendira, et al., Phys. Rev. Lett. 106 (2011) 080801.
[9] R.H. Parker, et al., Science 360 (2018) 191.
[10] M. Knecht, EPJ Web Conf. 179 (2018) 01008.
[11] J. Bijnens, E. Pallante, J. Prades, Phys. Rev. Lett. 75 (1995) 1447, Erratum: Phys. Rev. Lett. 75 (1995) 3781.
[12] J. Bijnens, E. Pallante, J. Prades, Nucl. Phys. B 474 (1996) 379.
[13] M. Hayakawa, T. Kinoshita, A.I. Sanda, Phys. Rev. Lett. 75 (1995) 790.
[14] M. Hayakawa, T. Kinoshita, A.I. Sanda, Phys. Rev. D 54 (1996) 3137.
[15] E. Bartos, et al., Nucl. Phys. B 632 (2002) 330.
[16] V. Pauk, M. Vanderhaeghen, Eur. Phys. J. C 74 (2014) 3008.
[17] G. Colangelo, M. Hoferichter, M. Procura, P. Stoffer, Phys. Rev. Lett. 118 (2017) 232001.
[18] G. Colangelo, M. Hoferichter, M. Procura, P. Stoffer, J. High Energy Phys. 1704 (2017) 161.
[19] G. Mennessier, Z. Phys. C 16 (1983) 241.
[20] G. Mennessier, S. Narison, W. Ochs, Phys. Lett. B 665 (2008) 205.
[21] G. Mennessier, S. Narison, X.-G. Wang, Phys. Lett. B 688 (2010) 59.
[22] G. Mennessier, S. Narison, X.-G. Wang, Phys. Lett. B 696 (2011) 40.
[23] R. Kaminski, G. Mennessier, S. Narison, Phys. Lett. B 680 (2009) 148.
[24] J. Aldins, T. Kinoshita, S.J. Brodsky, A.J. Dufner, Phys. Rev. D 1 (1970) 2378.
[25] M. Tanabashi, et al., Particle Data Group, Phys. Rev. D 98 (2018) 030001.
[26] R. Mertig, M. Bohm, A. Denner, Comput. Phys. Commun. 64 (1991) 345.
[27] V. Shtabovenko, R. Mertig, F. Orellana, Comput. Phys. Commun. 207 (2016) 432.
[28] M. Knecht, A. Nyffeler, Phys. Rev. D 65 (2002) 073034.
[29] J. Stern, B. Moussallam, arXiv:hep-ph/9404353.
[30] M. Knecht, B. Moussallam, J. Stern, Nucl. Phys. B 429 (1994) 125.
[31] J. Bijnens, E. Gamiz, E. Lipartia, J. Prades, J. High Energy Phys. 0304 (2003) 055.
[32] M. Knecht, A. Nyffeler, Eur. Phys. J. C 21 (2001) 659.
[33] F. Jegerlehner, A. Nyffeler, Phys. Rep. 477 (2009) 1.
[34] R.L. Jaffe, Phys. Rev. D 15 (1977) 267;
R.L. Jaffe, Phys. Rev. D 15 (1977) 281.
[35] N.N. Achasov, V.N. Ivanchenko, Nucl. Phys. B 315 (1989) 465;
N.N. Achasov, G.N. Shestakov, Nucl. Phys. B, Proc. Suppl. 225–227 (2012) 135.
[36] G. 't Hooft, et al., Phys. Lett. B 662 (2008) 424.
[37] H. Fritzsch, P. Minkowski, Nuovo Cimento A 30 (1975) 393.
[38] P. Minkowski, W. Ochs, Eur. Phys. J. C 9 (1999) 283;
P. Minkowski, W. Ochs, Eur. Phys. J. C 39 (2005) 71.
[39] V.A. Novikov, et al., Nucl. Phys. B 191 (1981) 301.
[40] S. Narison, G. Veneziano, Int. J. Mod. Phys. A 4 (1989) 2751.
[41] S. Narison, Nucl. Phys. B 509 (1998) 312.
[42] S. Narison, Phys. Rev. D 73 (2006) 114024.
[43] W. Ochs, J. Phys. G 40 (2013) 043001.
[44] E. Klempt, A. Zaitsev, Phys. Rep. 454 (2007) 1.
[45] V. Mathieu, N. Kochelev, V. Vento, Int. J. Mod. Phys. E 18 (2009) 1.
[46] V. Crede, C.A. Meyer, Prog. Part. Nucl. Phys. 63 (2009) 74.
[47] U. Gastaldi, M. Berretti, arXiv:1804.9121, 2018;
U. Gastaldi, Talk given at QCD18, 2–6 july 2018 (Montpellier).
[48] L. Gong, Nucl. Part. Phys. Proc. 294–296 (2018) 100;
H.-H. Liu, Nucl. Part. Phys. Proc. 294–296 (2018) 105.
[49] G. Wormser, Talk given at QCD18, 2–6 july 2018 (Montpellier).
[50] D. Alde, et al., Phys. Lett. B 201 (1988) 160;
D. Alde, et al., Nucl. Phys. B 269 (1988) 485.
[51] M.A. Shifman, A.I. Vainshtein, V.I. Zakharov, Nucl. Phys. B 147 (1979) 385.
[52] M.A. Shifman, A.I. Vainshtein, V.I. Zakharov, Nucl. Phys. B 147 (1979) 448.
[53] S. Narison, QCD as a theory of hadrons, Camb. Monogr. Part. Phys. Nucl. Phys. Cosmol. 17 (2002) 1, arXiv:hep-ph/0205006.
[54] S. Narison, QCD spectral sum rules, World Sci. Lect. Notes Phys. 26 (1989) 1.
[55] S. Narison, Phys. Rep. 84 (1982) 263.
[56] S. Narison, Riv. Nuovo Cimento 10 (2) (1987) 1.
[57] F.M. Renard, Basics of e^+e^- Collisions, Ed. Frontières, Gif sur Yvette, France, 1981.
[58] R.J. Crewther, Phys. Rev. Lett. 28 (1972) 1421.
[59] J. Ellis, M.S. Chanowitz, Phys. Rev. D 7 (1973) 2490.
[60] P. Di Vecchia, G. Veneziano, Nucl. Phys. B 171 (1981) 253.
[61] J. Ellis, J. Lanik, Phys. Lett. B 150 (1985) 289.
[62] For a general discussion, see the section on *Resonances* by D.M. Asner, C. Hanhart and E. Klempt in [25].
[63] S. Willenbrock, G. Valencia, Phys. Lett. B 259 (1991) 373.
[64] A. Sirlin, Phys. Rev. Lett. 67 (1991) 2127.
[65] R.G. Stuart, Phys. Rev. Lett. 70 (1993) 3193.
[66] H. Veltman, Z. Phys. C 62 (1994) 35.
[67] M. Passera, A. Sirlin, Phys. Rev. Lett. 77 (1996) 4146.
[68] B.A. Kniehl, A. Sirlin, Phys. Rev. Lett. 81 (1998) 1373.
[69] P.A. Grassi, B.A. Kniehl, A. Sirlin, Phys. Rev. Lett. 86 (2001) 389.
[70] I. Caprini, G. Colangelo, H. Leutwyler, Phys. Rev. Lett. 96 (2006) 132001.
[71] I. Caprini, G. Colangelo, J. Gasser, H. Leutwyler, Phys. Rev. D 68 (2003) 074006.
[72] F.J. Yndurain, R. Gracia-Martin, J.R. Pelaez, Phys. Rev. D 76 (2007) 074034.
[73] K.L. Au, D. Morgan, M.R. Pennington, Phys. Rev. D 35 (1987) 1633.
[74] M. Hoferichter, D.R. Phillips, C. Schat, Eur. Phys. J. C 71 (2011) 1743.
[75] B. Moussallam, Eur. Phys. J. C 7 (2011) 1814.
[76] E.L. Lomon, S. Pacetti, Phys. Rev. D 85 (2012) 113004, Erratum: Phys. Rev. D 86 (2012) 039901.
[77] B. Moussallam, Eur. Phys. J. C 73 (2013) 2539.
[78] M. Poppe, Int. J. Mod. Phys. A 1 (1986) 545.
[79] G. Colangelo, M. Hoferichter, M. Procura, P. Stoffer, J. High Energy Phys. 1509 (2015) 074.
[80] N.N. Achasov, G.N. Shestakov, Phys. Rev. D 81 (2010) 094029.
[81] J. Prades, E. de Rafael, A. Vainshtein, arXiv:0901.0306 [hep-ph], 2009.
[82] F. Jegerlehner, arXiv:1511.04473 [hep-ph].
[83] M. Davier, A. Hoecker, B. Malaescu, Z. Zhang, Eur. Phys. J. C 77 (12) (2017) 827.
[84] A. Keshavarzi, D. Nomura, T. Teubner, Phys. Rev. D 97 (2018) 114025 and references therein.
[85] J. Charles, D. Greynat, E. de Rafael, arXiv:1712.02202 [hep-ph], 2017.
[86] M. Benayoun, P. David, L. DelBuono, F. Jegerlehner, arXiv:1605.04474v1 [hep-ph].
[87] C.A. Dominguez, et al., arXiv:1707.07715v1 [hep-ph], 2017.
[88] F. Burger, et al., ETM collaboration, J. High Energy Phys. 1402 (2014) 099.
[89] B. Chakraborty, et al., HPQCD collaboration, Phys. Rev. D 96 (2017) 034516.
[90] Sz. Borsanyi, et al., BMW collaboration, arXiv:1711.04980 [hep-latt], 2017.
[91] M. Della Mote, et al., J. High Energy Phys. 1710 (2017) 020.
[92] T. Blum, et al., arXiv:1801.07224 [hep-latt], 2018.
[93] D. Giusti, F. Sanfilippo, S. Simula, arXiv:1808.00887 [hep-latt], 2018.
[94] A. Nyffeler, Phys. Rev. D 94 (2016) 053006.
[95] A. Guevara, P. Roig, J.J. Sanz-Cillero, J. High Energy Phys. 1806 (2018) 160;
J.J. Sanz-Cillero, Talk given at QCD18, 2–6 july 2018 (Montpellier).
[96] G.W. Bennett, et al., Muon g-2 Collaboration, Phys. Rev. D 73 (2006) 072003.
[97] T. Aoyama, M. Hayakawa, T. Kinoshita, M. Nio, Phys. Rev. Lett. 109 (2012) 111808.
[98] A. Kurz, et al., Phys. Rev. D 92 (2015) 073019.
[99] M. Knecht, S. Peris, M. Perrottet, E. de Rafael, J. High Energy Phys. 0211 (2002) 003.
[100] A. Czarnecki, W.J. Marciano, A. Vainshtein, Phys. Rev. D 67 (2003) 073006, Erratum: Phys. Rev. D 73 (2006) 119901.
[101] A. Kurz, T. Liu, P. Marquard, M. Steinhauser, Phys. Lett. B 734 (2014) 144.
[102] S. Narison, Phys. Lett. B 568 (2003) 231.